JVI Journals.ASM.org

Interactions between the Influenza A Virus RNA Polymerase Components and Retinoic Acid-Inducible Gene I

Weizhong Li, Hongjun Chen, Troy Sutton, Adebimpe Obadan, Daniel R. Perez

Department of Veterinary Medicine, University of Maryland, College Park, and Virginia-Maryland Regional College of Veterinary Medicine, College Park, Maryland, USA

ABSTRACT

The influenza A virus genome possesses eight negative-strand RNA segments in the form of viral ribonucleoprotein particles (vRNPs) in association with the three viral RNA polymerase subunits (PB2, PB1, and PA) and the nucleoprotein (NP). Through interactions with multiple host factors, the RNP subunits play vital roles in replication, host adaptation, interspecies transmission, and pathogenicity. In order to gain insight into the potential roles of RNP subunits in the modulation of the host's innate immune response, the interactions of each RNP subunit with retinoic acid-inducible gene I protein (RIG-I) from mammalian and avian species were investigated. Studies using coimmunoprecipitation (co-IP), bimolecular fluorescence complementation (BiFc), and colocalization using confocal microscopy provided direct evidence for the RNA-independent binding of PB2, PB1, and PA with RIG-I from various hosts (human, swine, mouse, and duck). In contrast, the binding of NP with RIG-I was found to be RNA dependent. Expression of the viral NS1 protein, which interacts with RIG-I, did not interfere with the association of RNA polymerase subunits with RIG-I. The association of each individual virus polymerase component with RIG-I failed to significantly affect the interferon (IFN) induction elicited by RIG-I and 5′ triphosphate (5′ppp) RNA in reporter assays, quantitative reverse transcription-PCR (RT-PCR), and IRF3 phosphorylation tests. Taken together, these findings indicate that viral RNA polymerase components PB2, PB1, and PA directly target RIG-I, but the exact biological significance of these interactions in the replication and pathogenicity of influenza A virus needs to be further clarified.

IMPORTANCE

RIG-I is an important RNA sensor to elicit the innate immune response in mammals and some bird species (such as duck) upon influenza A virus infection. Although the 5′-triphosphate double-stranded RNA (dsRNA) panhandle structure at the end of viral genome RNA is responsible for the binding and subsequent activation of RIG-I, this structure is supposedly wrapped by RNA polymerase complex (PB2, PB1, and PA), which may interfere with the induction of RIG-I signaling pathway. In the present study, PB2, PB1, and PA were found to individually interact with RIG-Is from multiple mammalian and avian species in an RNA-independent manner, without significantly affecting the generation of IFN. The data suggest that although RIG-I binding by RNA polymerase complex is conserved in different species, it does not appear to play crucial role in the modulation of IFN *in vitro*.

Influenza A virus is a member of the *Orthomyxoviridae* family and contains eight segments of negative-sense genomic RNA. Within the virus particle, viral RNAs (vRNAs) are wrapped with multiple copies of the nucleoprotein (NP) and are bound to a heterotrimeric polymerase complex composed of basic polymerases 1 and 2 (PB1 and PB2, respectively) and the acidic polymerase (PA) to collectively form viral ribonucleoprotein particles (vRNPs). Upon entry and uncoating, the vRNPs travel to the nucleus through interactions with importin-like factors and components of the nuclear pore complex. The vRNPs form the minimal units for transcription and replication of viral RNAs. PB2 recognizes and binds the methylated cap of cellular pre-mRNAs (1), and then PA cleaves the cap and generates 5′-capped RNA fragments (2), which are then used to prime viral mRNA transcription by PB1 (3). The accumulation of NP during infection is thought to favor the switching of viral RNA from transcription to replication (4) and promote the nuclear export of progeny vRNPs (in association with the viral proteins M1 and NEP and cellular factors) (5). The protein components of vRNPs are also involved in virulence, host adaptation, and interspecies transmission of influenza A virus, presumably due to interactions with numerous host factors (6).

The innate immune response, especially the interferon (IFN)-mediated response, makes up the first line of defense against the invasion of pathogens. The production of type I IFN is primarily induced by Toll-like receptors (TLRs) located in the endosome or cellular membrane and RIG-I like receptors (RLRs) distributed mainly in the cytoplasm. RIG-I has been identified as the major cellular sensor for IFN induction upon influenza virus infection (7, 8). RIG-I recognizes the 5′ triphosphate (5′ppp) in viral genomic RNAs (9, 10) or double-stranded RNA (dsRNA) intermediates synthesized during virus replication (7, 11). Recently, RIG-I was shown to preferentially associate with short subgenomic viral segments in infected cells (12). Binding to its ligand induces a conformational change in RIG-I that leads to the ubiquitination of CARD domains (caspase activation and recruitment domains) by TRIM25 (tripartite motif protein 25) or ubiquitina-

Received 12 May 2014 **Accepted** 12 June 2014

Published ahead of print 18 June 2014

Editor: M. S. Diamond

Address correspondence to Daniel R. Perez, dperez1@umd.edu.

doi:10.1128/JVI.01383-14

tion of C-terminal regulatory domain by Riplet (RING finger protein leading to RIG-I activation) and the subsequent complex formation between RIG-I and IPS-1 (beta interferon promoter stimulator 1, also known as MAVS, VISA, or Cardif) on the surface of the mitochondria (13). The ensuing signal cascade causes the nuclear translocation of IRF3, IRF7, ATF-2/c-Jun, and NF-κB, which activate the IFN-β promoter and promote the expression of IFN (14). Finally, hundreds of interferon-stimulated genes (ISGs), such as those encoding PKR, 2′,5′-OAS, Mx1, and ADAR1, among others, are produced and exert their antiviral function via multiple mechanisms (15). Of note, RIG-I has been found not only in humans and mammals but also in a wide variety of other animal species, such as zebrafish, amphibians, and birds (16, 17). Interestingly, Galliformes (e.g., chickens) appear to have lost through evolution the gene that encodes RIG-I, although it is maintained in other avian species such as in Anseriformes (ducks and geese) (18, 19). This difference has been suggested as a possible explanation for the increased susceptibility of chickens compared to that of ducks to highly pathogenic influenza viruses (18).

To survive in host cells, influenza A viruses have evolved various strategies to circumvent the IFN response. The NS1 protein, a nonstructural protein generated during the early stages of virus infection, is a well-characterized IFN inhibitor (20). NS1 can limit IFN induction by various strategies, including (i) sequestration of viral dsRNA away from host-encoded RNA sensors (21), (ii) formation of complexes with RIG-I (9, 10, 22), (iii) suppression of TRIM25- and/or Riplet-mediated RIG-I ubiquitination (16, 22), and (iv) blocking of cellular pre-mRNA processing and transport and thus decreasing synthesis of antiviral proteins involved in innate immunity (23, 24). Apart from NS1, other influenza virus proteins also possess IFN-antagonizing capabilities. PB1-F2 can act on MAVS (25, 26) and/or interfere with the RIG-I/MAVS protein complex (27), thereby inhibiting IFN production. In addition, the PB2 protein (28, 29) from human influenza A virus alone or in the context of the three viral polymerase subunits has been shown to interact with MAVS and impair host antiviral responses mediated by IFN (30).

In the present study, evidence was obtained for the direct interactions of viral RNA polymerase components from an avian influenza A virus (H9N2 subtype) with RIG-I from various host species (human, duck, mouse, and swine). NP was also shown to interact with RIG-I, although this interaction is indirect and mediated by RNA. Association of virus RNP subunits with RIG-I did not remarkably contribute to the inhibition of the IFN signaling pathway. Collectively, these findings highlight the interactions of viral polymerase components with RIG-I, although the biological significance of these interactions awaits clarification.

MATERIALS AND METHODS

Cells and viruses. Madin-Darby canine kidney (MDCK) cells, chicken embryonic fibroblasts (DF1), duck embryonic fibroblasts (CCL-141), a mouse macrophage cell line (RAW264.7), a swine epithelial cell line (PK15), a human embryonic kidney cell line (293T), a human lung carcinoma cell line (A549), and African green monkey kidney (Vero) cells were cultured in OPTI-MEM supplemented with antibiotics and 10% fetal calf serum at 37°C in 5% CO_2. Influenza A virus strain A/Guinea Fowl/Hong Kong/WF10/99 (H9N2) (WF10) has been previously described (31). The virus was propagated in 9-day-old embryonated eggs. Virus titer was determined by 50% tissue culture infective dose ($TCID_{50}$) in MDCK cells using the method of Reed and Muench (32).

Plasmids. To construct plasmids used for biomolecular fluorescence complementation (BiFc) analysis, the sequences encoding the N terminus of enhanced yellow fluorescent protein (EYFP; containing residues 1 to 155 and a Q70M point mutation to enhance stability of fluorescence signal; NYFP), the C terminus of EYFP (comprising residues 156 to 239; CYFP), or the N terminus of Cerulean (a variant of EYFP) corresponding to residues 1 to 173 (NCe) were fused to PB2, PB1, PA, or NP at the C-terminal end via a linker (three repeats of the peptide sequence GGG GS). The chimeric genes were then cloned into the pDP2002 or pcDNA3 vector to yield plasmids pDPPB2-NYFP, pDPPB1-NYFP, pDPPA-NYFP, pDPNP-NCe, pDPPB2-CYFP, pDPPA-CYFP, pc-PB2-NYFP, pc-PB1-NYFP, pc-PA-NYFP, and pc-NP-NYFP. Plasmid pcDNA3-NYFP was constructed via the insertion of NYFP-encoding sequence into pcDNA3. Based on this plasmid, a derivative construct was produced, pc-WFNS1(ΔS)-NYFP, which expresses NS1 protein (without a splicing site) flanked by a linker-NYFP segment at the C terminus. The full-length of RIG-I open reading frame (ORF) from different species (duck, mouse, swine, or human) was amplified from WF10 virus-infected or polyI·C-stimulated cells (CCL-141, RAW264.7, PK15, or A549) using overlapping PCR. Different RIG-I genes were then ligated with pCMV-Flag-MAT-Tag-1 vector (abbreviated pflag vector; Sigma, St. Louis, MO) or pCMV-3Tag-2b vector (abbreviated pmyc-2b; Agilent Technologies, La Jolla, CA) to produce plasmids pflag-DRIG, pflag-MRIG, pflag-SRIG, pflag-HRIG, and pmyc-HRIG. The RIG-I genes were cloned into the pcDNA3 vector, and the linker-CYFP sequence was subsequently inserted into these constructs to produce plasmids pc-DRIG-CYFP, pc-MRIG-CYFP, pc-SRIG-CYFP, and pc-HRIG-CYFP, respectively. Using this strategy, recombinant plasmids pc-DRIG-NYFP, pc-MRIG-NYFP, pc-SRIG-NYFP, and pc-HRIG-NYFP were also generated; all these plasmids contain a linker and an N-terminal EYFP sequence with a Q70M point mutation.

To construct plasmids used for coimmunoprecipitation (co-IP), confocal microscopy, and IRF3 phosphorylation assays, the PB2, PB1, PA, or NP gene from WF10 virus was amplified by reverse transcription-PCR (RT-PCR) and inserted in-frame into pCMV-3Tag-2a vector (termed pmyc-2a vector; Agilent Technologies). The corresponding plasmids encode myc-tagged recombinant proteins and were labeled pmyc-PB2, pmyc-PB1, pmyc-PA, and pmyc-NP, respectively. In addition, the PB2, PB1, PA, and NP genes were also fused with pcDNA3 vector, generating plasmids pcDNA3-PB2, pcDNA3-PB1, pcDNA3-PA, and pcDNA3-NP, respectively. Reporter plasmid pGluc-IFNβ, which carries the *Gaussia* luciferase gene under the control of human IFN-β promoter, was created by cloning the human IFN-β promoter (nucleotide [nt] −125 ~ +19) into pGluc-basic vector (New England BioLabs, Ipswich, MA). Another reporter plasmid, pISRE-Luc, was obtained from Agilent Technologies. Two negative-control plasmids, pflag-GFP and pmyc-GFP, were obtained by fusing the gene encoding enhanced green fluorescent protein (EGFP) with the corresponding epitopes in pflag or pmyc-2a vectors via cloning into the BamHI site.

To produce reverse genetics plasmid pDPNS2 (lacking the NS1 gene), the pDPNS-WF10 plasmid was used as a template and inverse PCR was performed first to remove the intron of the NS1 gene. Subsequently, the PCR product was digested by BsmBI and self-ligated. Plasmid pCAGGS-WFNS1(ΔS), encoding NS1 protein from WF10 virus, was generated by the fusion of the NS1 ORF with the pCAGGS vector. The splicing site in the NS1 ORF had been deleted via point mutations. Plasmid pCAGGS-GST, which served as a negative control, was constructed by the insertion of the glutathione S-transferase (GST) ORF into the pCAGGS vector via EcoRI and BglII sites. pflag-IRF3, a recombinant plasmid used for IRF3 phosphorylation analysis, was generated via the insertion of the full-length ORF of human IRF3 into pflag vector at the KpnI site. All plasmid constructs were verified by Sanger sequencing using appropriate primers and a 3500×L genetic analyzer from Applied Biosystems (Foster City, CA).

Co-IP. Confluent 293T cells seeded in 10-cm dishes were transfected with different combinations of plasmids. After 48 h of cotransfection by the indicated plasmids (or after 32 h of transfection followed by 14 h of infection with the WF10 virus), cells were lysed in cold 0.5% NP-40 lysis buffer at 4°C for 30 min and then centrifuged at 14,000 × *g* for 10 min. Supernatants were collected and divided into two parts; one part was supplied with RNase A (Invitrogen, Carlsbad, CA) at a final concentration of 100 μg/ml, while the other part was kept untreated. After 1 h of rotation of the samples at 4°C and 10 min of centrifugation at 14,000 × *g*, supernatants were harvested and precleared with Dynabeads-protein G (Invitrogen) at 4°C for 4 h. Meanwhile, 5 μl of mouse anti-myc antibody (Cell Signaling Technology, Danvers, MA) or mouse anti-Flag antibody (Sigma, St. Louis, MO) was mixed with Dynabeads-protein G at room temperature for 1 h and at 4°C for 3 h to allow the binding of antibody to the beads. Supernatants were subsequently incubated overnight with antibody-coated beads at 4°C with gentle rotation. After washing 4 times with radioimmunoprecipitation assay (RIPA) lysis buffer for 5 min each time, the precipitated proteins were eluted from beads with hot Laemmli sample buffer at 100°C for 7 min and resolved by 4 to 20% or 7.5% SDS-PAGE. Rabbit anti-Flag antibody (Sigma; 1:500), mouse anti-myc antibody (Cell Signaling Technology; 1:1,000), goat anti-PB2 antibody (Santa Cruz, CA; 1:200), goat anti-PB1 antibody (Santa Cruz; 1:150), rabbit anti-PA antibody (GeneTex, San Antonio, TX; 1:2,000), and rabbit anti-NP antibody (Novas Biologicals, Littleton, CO; 1:2,000) as well as peroxidase-conjugated secondary antibody (Southern Biotech, Birmingham, AL; 1:4,000) were used to probe the eluted proteins. Ten percent of cell lysates was kept as input samples and subjected to Western blotting using the antibodies mentioned above.

SDS-PAGE and Western blotting. Cells were harvested and lysed with 2× Laemmli sample buffer at 100°C for 7 min. After brief sonication, the lysates were separated on a 4 to 20% gradient polyacrylamide gel or 7.5% polyacrylamide gel (Bio-Rad, Hercules, CA) and transferred to a nitrocellulose membrane, followed by blocking in Tris-buffered saline (TBS) solution containing 0.1% Tween 20 and 5% nonfat milk for 2 h. The membrane was incubated overnight at 4°C with the desired antibodies. After being washed three times with TBS containing 0.1% Tween 20, the membrane was exposed to peroxidase-conjugated secondary antibody (Southern Biotech; 1:4,000 dilution) for 2 h at room temperature. Immunoreactive proteins were visualized using West Pico enhanced chemiluminescence reagent (Pierce, Rockford, IL) and autoradiography.

BiFc analysis. Tissue culture cells grown on 12-well plates were transfected with the selected pairs of bimolecular fluorescence complementation (BiFc) constructs (1 μg of each plasmid) using Transfectin (Bio-Rad, Hercules, CA) (for MDCK cells) or Transit-LT1 (Mirus, Madison, WI) (for 293T and DF1 cells) by following the procedures provided by the manufacturers. At 24 h posttransfection (hpt), cells were further subjected to 14 h of incubation at 30°C. Then the cells were fixed with 4% paraformaldehyde for 10 min and permeabilized with 0.2% Triton X-100 for 7 min, followed by 10 min of nuclear staining with 4′,6-diamidino-2-phenylindole (DAPI; Thermo Scientific, Rockford, IL; 1:500). The digitized images were captured using a Zeiss SM510 confocal microscope (Carl Zeiss Microscopy, Thornwood, NY). ImageJ software was used to quantitate the frequency and intensities of BiFc signals if necessary.

Immunofluorescence analysis. RNP subunit-expressing plasmids were introduced into 293T cells grown on coverslips along with different RIG-I plasmids by Transit-LT1 reagent. Twenty-four hours later, cells were subjected to 10 min of fixation with 4% paraformaldehyde and 7 min of permeabilization with 0.2% Triton X-100. After blocking for 40 min in phosphate-buffered saline (PBS) containing 3% bovine serum albumin (BSA), cells were stained with rabbit anti-Flag antibody (Sigma; 1:300) and mouse anti-myc antibody (Cell Signaling Technology; 1:700) diluted in 3% BSA-PBS for 2 h. Then the cells were washed 3 times with PBS and incubated with Alexa Fluor 568-conjugated donkey anti-rabbit antibody (Invitrogen, Carlsbad, CA; 1:300) and Alexa Fluor 488-conjugated donkey anti-mouse antibody (Invitrogen; 1:300) for 1 h. Nuclei were stained with DAPI (Thermo Scientific; 1:500) for 10 min, and the samples were visualized using a Zeiss SM510 confocal microscope. Digital images were processed with ZEN software.

Generation of NS1-deleted influenza virus. TheNS1-deleted WF10 virus was rescued in Vero cells. In brief, Vero cells (95% confluent) were transfected with plasmid pDPNS2 along with reverse genetics plasmids encoding seven other segments of WF10 virus using Transfectin reagent. At 24 hpt, the medium was replaced by serum-free medium containing 1 μg/ml of tosylsulfonyl phenylalanyl chloromethyl ketone (TPCK)-trypsin. TPCK-trypsin was supplied every day at a final concentration of 1 μg/ml until cytopathic effect was observed. The virus was propagated in 7-day-old eggs and titrated by $TCID_{50}$ in MDCK cells. To verify whether the virus lacked NS1, Sanger sequencing and Western blot analyses were performed.

Localization of endogenous RIG-I during transfection or infection. A549 cells were transfected with appropriate plasmids (pmyc-PB2, pmyc-NP, or pmyc empty vector) for 24 h or infected with viruses (wild-type or NS1-deleted WF10 virus) for 14 h at a multiplicity of infection (MOI) of 5. Immunofluorescence assays (IFAs) were then performed as described above using rabbit anti-RIG-I antibody (Santa Cruz; 1:30) and mouse anti-myc antibody (Cell Signaling Technology; 1:250) or mouse anti-NP antibody (Santa Cruz; 1:250), followed by staining with Alexa Fluor 488-conjugated donkey anti-rabbit antibody (Invitrogen; 1:250) and Alexa Fluor 568-conjugated donkey anti-mouse antibody (Invitrogen; 1:300). To investigate the location dynamics of endogenous RIG-I in the whole infection process, A549 cells were infected with wild-type or NS1-deleted WF10 virus at an MOI of 5. At 1, 2, 4, 6, 8, 10, 12, and 14 hours postinfection (hpi), cells were fixed with 4% paraformaldehyde and permeabilized with 0.2% Triton X-100. RIG-I was probed with rabbit anti-RIG-I antibody (Santa Cruz; 1:30) and Alexa Fluor 488-conjugated donkey anti-rabbit antibody (Invitrogen; 1:250).

Nuclear and cytosolic fractionation assay. Nuclear and cytosolic proteins were extracted from virus-infected A549 cells at various time points postinfection using the NE-PER nuclear and cytoplasmic extraction kit (Pierce) according to the manufacturer's instructions. Briefly, the cells in 12-well plates were suspended with 100 μl of CER I and incubated for 10 min on ice. Then, the cells were mixed with 5.5 μl of CER II and centrifuged for 5 min at 13,000 × *g* after 1 min of incubation on ice. Supernatants (cytoplasmic fraction) were collected immediately and stored at −20°C. The pellets were resuspended with 25 μl of NER and maintained on ice for 40 min while being vortexed for 15 s at 10-min intervals. Nuclear proteins were harvested after 10 min of centrifugation at 13,000 × *g* to discard the insoluble components. Nuclear and cytosolic fractions were subsequently subjected to SDS-PAGE and Western blot analysis using rabbit anti-RIG-I antibody (Santa Cruz; 1:1500), rabbit antitubulin antibody (Sigma; 1:1,000), rabbit anti-PCNA antibody (Cell Signaling Technology; 1:1,000), or rabbit anti-NP antibody (Novas Biologicals; 1:2,000).

IFN-β and interferon-stimulated response element (ISRE) promoter stimulation assays. 293T cells in 24-well plates were transfected with various amounts of pGluc-IFNβ-, pCMV/SEAP-, pflag-HRIG-, and pcDNA3-based expression plasmids for PB2, PB1, PA, and NP, respectively. Plasmid pCAGGS-WFNS1(ΔS) was used as a positive control. Empty pcDNA3 vector was added to ensure that the total amount of plasmid was the same for each well. Cells were incubated for 24 h, followed by transfection of 5′ppp RNA (Invivogen, San Diego, CA; 0.5 μg/well) using Lipofectamine 2000 (Invitrogen). At 24 h after stimulation with 5′ppp RNA, supernatants were harvested and analyzed for both luciferase (Gluc) and secreted alkaline phosphatase (SEAP) activities using the Bio-Lux *Gaussia* luciferase assay kit (New England BioLabs, Ipswich, MA) and the Phospha-Light secreted alkaline phosphatase reporter gene kit (Applied Biosystems) according to the manufacturers' directions. All experiments were repeated independently three times, and the relative IFN-β promoter activities were expressed as the average values of Gluc normalized to SEAP.

For ISRE activity analysis, pISRE-Luc plasmids were introduced into

293T cells in combination with pflag-HRIG (or empty pflag vector) and plasmid pcDNA3-PB2, pcDNA3-PB1, pcDNA3-PA, pcDNA3-NP, or pCAGGS-WFNS1(ΔS) or empty pcDNA3 vector. 5′ppp RNA was administered at a concentration of 0.5 μg/well via transfection. At 24 hpt, the supernatants were collected for SEAP detection as described above. At the same time, the cells were lysed for determination of firefly luciferase activity using the Bright-Glo luciferase assay kit from Promega. Experiments were performed in triplicate, and the relative ISRE activity was expressed as the ratio of Luc to SEAP.

Quantitative RT-PCR (qRT-PCR). 293T cells in 12-well plates were transfected with the desired plasmids using Transit-LT1. Twenty-four hours later, the cells were further transfected with 1 μg of 5′ppp RNA (Invivogen) using Lipofectamine 2000. In another group, RNA extracted from WF10 virus-infected or mock-infected Vero cells was used as a stimulator (1 μg/well). Total RNA was isolated from cells using the RNeasy minikit (Qiagen, Valencia, CA) after 11 h of stimulation and treated with DNase I to prevent the contamination of DNA. The cDNA was synthesized using oligo(dT) primer and the SuperScript III First-Strand Synthesis kit (Invitrogen). PCR was performed in a volume of 20 μl for 40 cycles (95°C for 10 s, 58°C for 20 s, and 72°C for 25 s) using the LightCycler 480 SYBR green I master mix kit (Roche, Indianapolis, IN). The primer sets we used were forward primer 5′-GATTCATCTAGCACTGGCTGG-3′ plus reverse primer 5′-CTTCAGGTAATGCAGAATCC-3′ for IFN-β and forward primer 5′-CCAAGGCCAACCGCGAGAAGATGAC-3′ plus reverse primer 5′-AGGGTACATGGTGGTGCCGCCAGAC-3′ for β-actin. The fluorescence signals were monitored by the LightCycler 480 real-time PCR system (Roche), and the specificity of PCR products was confirmed by melting-curve analysis. The mRNA expression levels of IFN-β relative to β-actin were determined by the threshold cycle ($2^{-\Delta\Delta CT}$) method.

Phosphorylation of IRF3. After 24 h of transfection of appropriate plasmids encoding RIG-I, IRF3, and myc-tagged viral proteins, 293T cells were stimulated with 5′ppp RNA (via transfection) for 12 h and lysed with Laemmli buffer supplied with phosphatase inhibitor. Cellular lysates were separated in an SDS-PAGE gel, following by immunoblotting using antibodies targeting phospho-IRF3 (Ser396) (Cell Signaling Technology; 1:1,000), total IRF3 (Cell Signaling Technology; 1:1,000), RIG-I (Santa Cruz; 1:2,000), myc (Cell Signaling Technology; 1:1,000), and glyceraldehyde-3-phosphate dehydrogenase (GAPDH; Santa Cruz; 1:3,000). The protein band intensities of phosphorylated IRF3 and total IRF3 were quantitated with ImageJ software.

Statistical analyses. Experimental data were expressed as means ± standard deviations (SD) and analyzed by GraphPad Prism 5 software (La Jolla, CA). One-way analysis of variance (ANOVA) was used, followed by the Dunnett *t* test. A *P* value of <0.05 was considered statistically significant.

RESULTS

Association between RNP subunits and RIG-I. To explore the possible interactions among RNP subunits and RIG-I, co-IP tests were performed. The Flag-tagged human RIG-I (Flag-HRIG) and myc-tagged PB2, PB1, PA, or NP were coexpressed in 293T cells. The myc-GFP expression plasmid was used as a negative control. RNase A treatment was used to evaluate the effect of RNA on the binding of RNP subunits with RIG-I. As shown in Fig. 1A, RNase A treatment completely degraded RNA extracted from cells. Regardless of RNase A treatment, Flag-HRIG could be pulled down by the myc antibody from cells coexpressing either myc-PB2, myc-PB1, or myc-PA but not from cells coexpressing myc-GFP (Fig. 1B), suggesting direct and RNA-independent interactions between RNA polymerase subunits and human RIG-I. In contrast, Flag-HRIG interaction with myc-NP was RNA dependent, since RNase A treatment entirely abolished the binding of myc-NP with Flag-HRIG (Fig. 1C). Of note, the interactions of RNP subunits with RIG-I were not limited to the human homolog, as similar interactions were observed with constructs encoding duck, mouse, and swine RIG-I (Fig. 1D to G), despite sharing 52.6%, 77.0%, and 78.1% amino acid homology with the human counterpart, respectively. These findings indicate that the binding of RNP subunits with RIG-I from different species may be an inherent property of RIG-I and reflects the evolutionary conservation of this intracellular RNA sensor.

BiFc is a simple and reliable technique to study protein-protein interactions. Two split fluorescent segments (e.g., N terminus of EYFP or C terminus of EYFP) are fused to two candidate proteins. If the candidate proteins interact with each other, the split fluorescent segments will form a complex and emit a fluorescent signal (33). In this study, the N-terminal 155 residues of the Q70M EYFP variant (NYFP), the N-terminal 173 residues of another variant, Cerulean EYFP (NCe), or the C-terminal 84 residues of EYFP (CYFP) were used to produce chimeric constructs with target proteins (PB2, PB1, PA, and NP) from the WF10 (31) virus or with RIG-I. Since previous studies showed that N-terminal fusion of GFP to either PB1 or PA severely altered the function of these proteins, while C-terminal fusion had no adverse effects (34, 35), all split fluorescent segments were placed on the C terminus of target proteins (Fig. 2A). Additionally, a short linker sequence with three repeats of GGGGS was inserted between the target proteins and the split fluorescent segments to ensure flexibility and accessibility of each protein product within the construct. The putative interactions between different target proteins facilitate the formation of NYFP/CYFP or NCe/CYFP complexes, which can produce stable fluorescence.

To test the associations between RNP subunits of influenza A virus and RIG-I, different combinations of BiFc plasmids were transfected into 293T cells. Obvious fluorescence was observed when HRIG-CYFP (human RIG-I fused to CYFP) and either PB2-NYFP, PB1-NYFP, PA-NYFP, or NP-NCe was coexpressed in the same cells (Fig. 2B). Compared with the fluorescent signals caused by HRIG-CYFP/PA-NYFP and HRIG-CYFP/NP-NCe, the signal intensities that resulted from HRIG-CYFP/PB2-NYFP and HRIG-CYFP/PB1-NYFP are relatively weaker (Fig. 2B), which can be attributed to the lower abundance of PB2-NYFP and PB1-NYFP relative to that of PA-NYFP and NP-NCe (Fig. 2F). Interestingly, fluorescence produced by HRIG-CYFP/PB2-NYFP as well as HRIG-CYFP/NP-NCe was predominantly nuclear, whereas fluorescence generated by HRIG-CYFP/PB1-NYFP as well as HRIG-CYFP/PA-NYFP had mostly a cytoplasmic distribution (Fig. 2B). Expression of RIG-I and individual vRNP protein components in single-plasmid transfection studies (data not shown) showed that (i) RIG-I located nearly exclusively in the cytoplasm, (ii) PB1 and PA were present in the cytoplasm at high concentrations and in the nucleus at low concentrations, and (iii) PB2 and NP predominantly distributed in the nucleus. Consistent with these results, RIG-I has already been shown to be a cytoplasmic protein (36), and individually expressed PB1 or PA was shown previously to display more cytoplasmic distribution than nuclear localization (35, 37). Thus, it is conceivable that the associations between RIG-I and PB1 or PA most probably occur in the cytoplasm. In contrast, since PB2 and NP contain strong nuclear targeting sequences (38, 39), they may bind RIG-I and sequester the latter in the nuclear compartment (Fig. 2B).

Since initial BiFc assays were performed using clones from the reverse genetics vector pDP2002, which is able to produce viral RNA simultaneously, it was important to exclude the potential

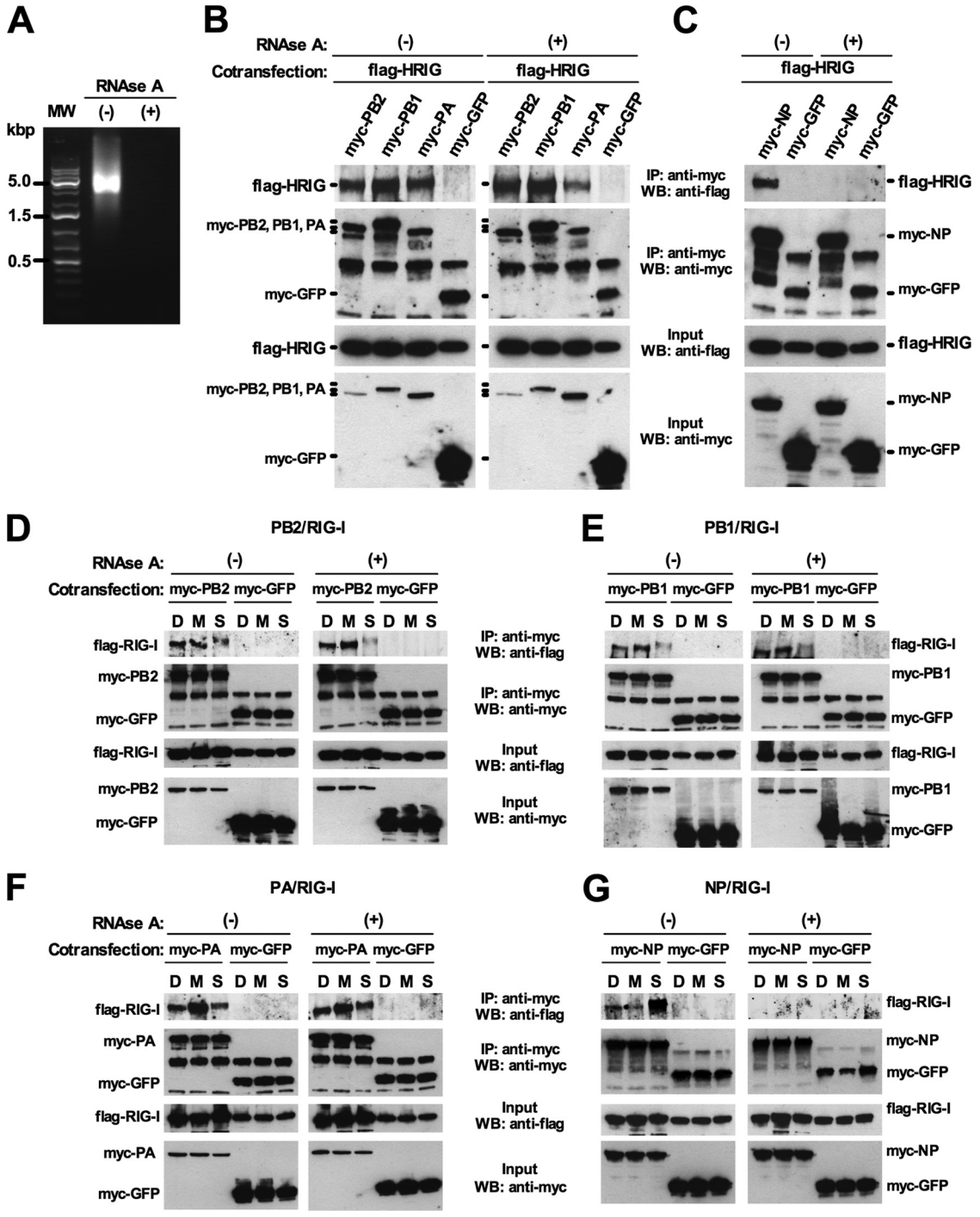

FIG 1 Interactions of viral RNP subunits with various RIG-Is in the presence or absence of RNA. (A) Degradation of cellular RNA by RNase A. (A) Cellular lysates from 293T cells were treated with RNase A (100 μg/ml) for 1 h at 4°C and subjected to agarose electrophoresis. MW, 1-kb DNA ladder. (B) RNA-independent interactions of PB2, PB1, and PA with human RIG-I (HRIG). 293T cells were transfected for 48 h with Flag-HRIG plasmid along with myc-tagged expression plasmids for PB2, PB1, PA, or GFP. After lysis with NP-40 buffer, the cellular lysates were left untreated [(−)] or treated for 1 h with RNase A [(+)]. Ten percent of cellular lysates was kept as input samples. The remaining cellular lysates were coimmunoprecipitated (co-IP) with mouse anti-myc antibody. Precipitated proteins were subjected to Western blot (WB) analysis using rabbit anti-Flag antibody or mouse anti-myc antibody. (C) RNase A treatment abolished the interaction between NP and human RIG-I. 293T cells were transfected with the indicated plasmids and lysed with NP-40 buffer, followed by RNase A digestion as indicated. Co-IP and WB were then conducted as described above. (D to G) Effect of RNase A treatment on the binding of each RNP component with RIG-I from duck, mouse, and swine. 293T cells were transfected for 48 h with plasmids expressing Flag-RIG-I from either duck (D), mouse (M), or swine (S) along with myc-tagged expression plasmids for PB2, PB1, PA, NP, or GFP. Co-IP and WB were then conducted as described above.

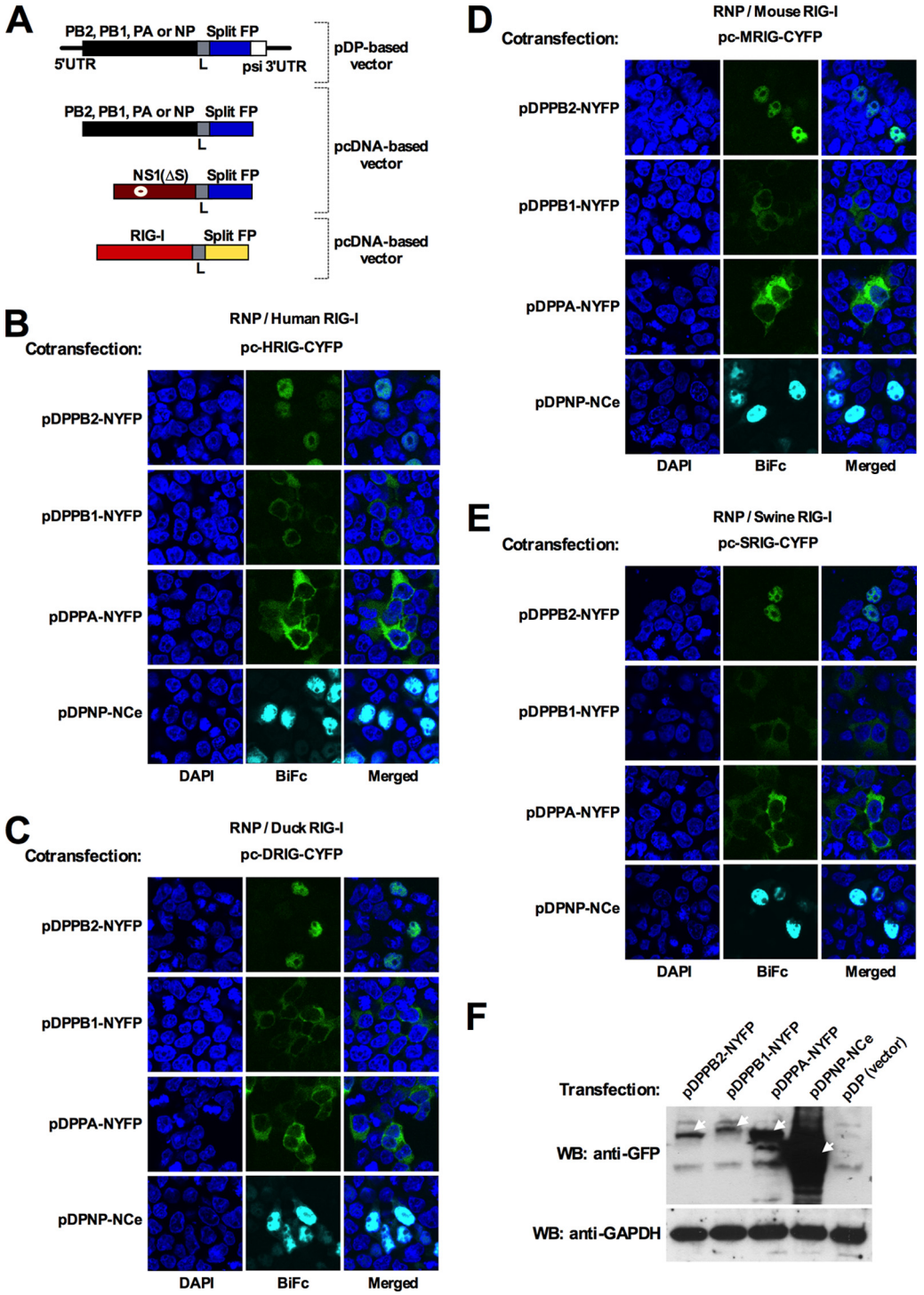

FIG 2 Association of vRNP components with different RIG-Is in BiFc analysis. (A) Schematic diagram of BiFc plasmids used in this study. The split fluorescence protein-encoding sequences were fused with the full-length ORFs of PB2, PB1, PA, NP, and NS1 from A/Guinea Fowl/Hong Kong/WF10/99 (H9N2) (WF10) virus via a linker (L, amino acids linker with three repeats of GGGGS) and cloned into plasmid pDP2002 (pDP based) or eukaryotic expression plasmid pcDNA3 (pcDNA based) to yield different BiFc plasmids. 5′UTR and 3′UTR, 5′ and 3′ untranslated regions of WF10 virus; psi, packaging signal; Split FP, NYFP, CYFP, or NCe constructs; NYFP, N terminus (residues 1 to 155) of EYFP with a Q70M point mutation; CYFP, C terminus (residues 156 to 239) of EYFP; NCe, N terminus (residues 1 to 173) of Cerulean (a variant of EYFP); NS1(ΔS), NS1-encoding sequence from WF10 virus with point mutations to delete the splicing site in NS1. (B) BiFc analysis of the association between RNP subunits from WF10 virus (pDP based; NYFP or NCe chimeras) and human RIG-I (HRIG-CYFP). The indicated plasmids were cotransfected into 293T cells. After 24 h of incubation at 37°C and 14 h of incubation at 30°C, the cells were fixed, stained with DAPI, and visualized with a Zeiss SM510 confocal microscope. (C to E) Association of individual RNP components (as NYFP or NCe chimeras) with RIG-I from duck (DRIG-CYFP), mouse (MRIG-CYFP), or swine (SRIG-CYFP). (F) Expression levels of different BiFc plasmids. 293T cells were transfected with indicated plasmids (based on the pDP2002 vector). At 36 h posttransfection, the cells were lysed and subjected to Western blot analysis using GFP or GAPDH antibody. Arrows indicate the expression of specific chimeric viral protein bands.

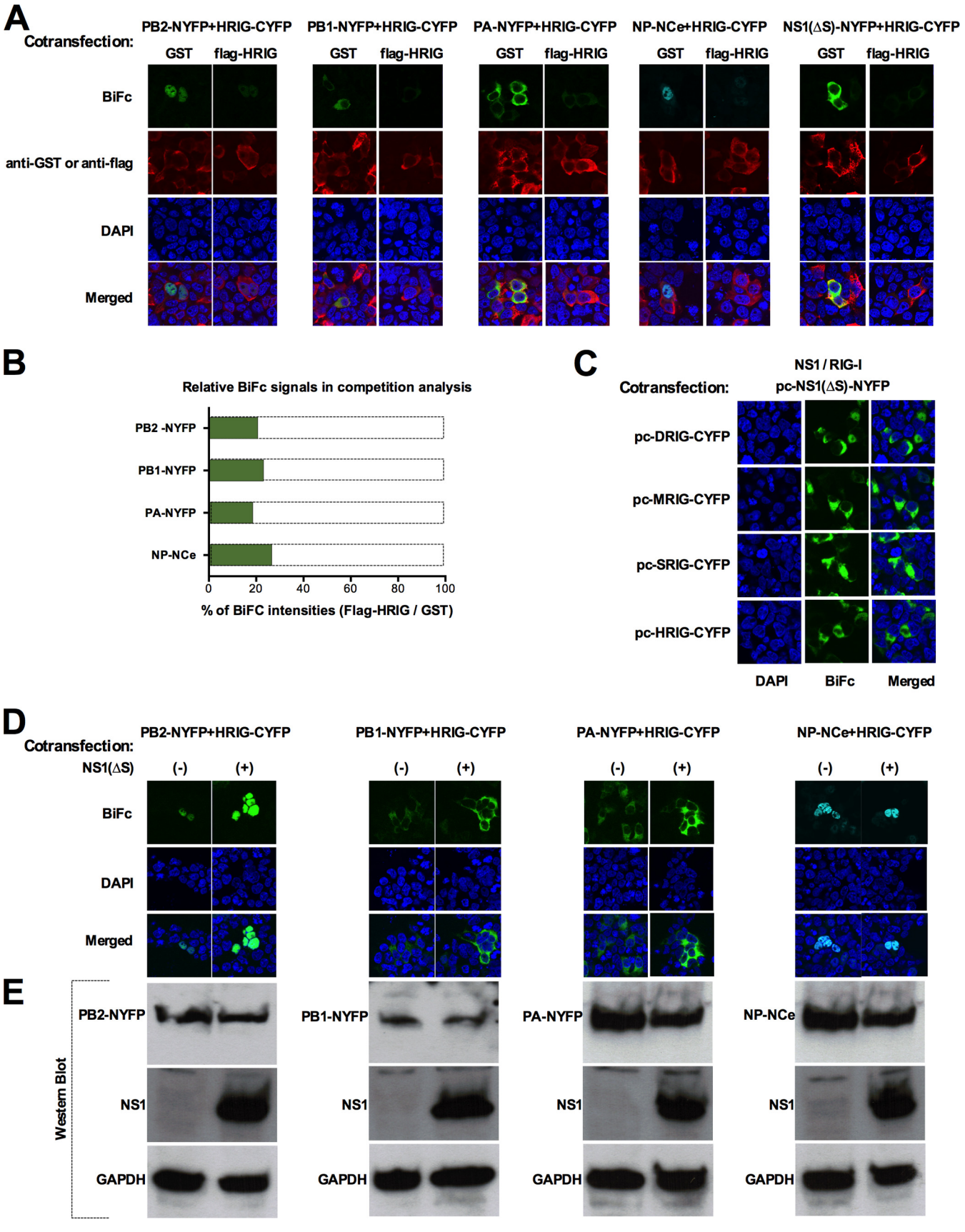
A
Cotransfection:
PB2-NYFP+HRIG-CYFP
PB1-NYFP+HRIG-CYFP
PA-NYFP+HRIG-CYFP
NP-NCe+HRIG-CYFP
NS1(ΔS)-NYFP+HRIG-CYFP
GST
flag-HRIG
BiFc
anti-GST or anti-flag
DAPI
Merged
B
Relative BiFc signals in competition analysis
PB2 -NYFP
PB1-NYFP
PA-NYFP
NP-NCe
0
20
40
60
80
100
% of BiFC intensities (Flag-HRIG / GST)
C
NS1 / RIG-I
Cotransfection:
pc-NS1(ΔS)-NYFP
pc-DRIG-CYFP
pc-MRIG-CYFP
pc-SRIG-CYFP
pc-HRIG-CYFP
DAPI
BiFc
Merged
D
Cotransfection:
PB2-NYFP+HRIG-CYFP
PB1-NYFP+HRIG-CYFP
PA-NYFP+HRIG-CYFP
NP-NCe+HRIG-CYFP
NS1(ΔS)
(-)
(+)
BiFc
DAPI
Merged
E
Western Blot
PB2-NYFP
PB1-NYFP
PA-NYFP
NP-NCe
NS1
GAPDH

participation of vRNA in the association of each vRNP component with RIG-I. Thus, four additional BiFc plasmids expressing RNP proteins but not vRNA were constructed based on the vector pcDNA3 (Fig. 2A). In the context of this new set of plasmids, BiFc signals were observed which were indistinguishable from those described above, suggesting direct associations of viral components with RIG-I in the absence of viral RNA. Similar interactions of RNP subunits with RIG-I were also observed for the duck, mouse, and swine homologs (Fig. 2C to E).

A major concern about BiFc analysis is the nonspecific signals resulting from random collision and self-assembly of the split fluorescent segments, especially at high expression levels (40–42). To exclude the possible false-positive results in BiFc analysis, an appropriate negative control is needed. Following the suggestion of Kodama and Hu (43) and approaches used by others (44, 45), we performed a competition assay to establish whether the fluorescence observed reflects a specific interaction. To this end, a Flag-tagged HRIG plasmid (or an irrelevant GST-expressing plasmid) was introduced into the cells in relatively larger amounts together with two chimeric protein plasmids carrying split fluorescent segments (HRIG-CYFP and PB2-NYFP, HRIG-CYFP and PB1-NYFP, HRIG-CYFP and PA-NYFP, or HRIG-CYFP and NP-NCe). As expected, the existence of a competitor (Flag-HRIG) remarkably inhibited the fluorescent signals compared with the unrelated protein GST (Fig. 3A). The average intensities of BiFc signals in the Flag-HRIG group after quantitation are only about 20% of that in the control (GST) group (Fig. 3B), implying that the interactions among RNP subunits and human RIG-I are specific.

NS1 does not negatively affect interaction between RNP subunits and RIG-I. Previous studies showed that the NS1 protein counteracts innate immune responses via multiple mechanisms (20) and that the direct interaction between NS1 and human RIG-I enhances virus replication (46–48). In this study, the association between NS1 and human RIG-I was also confirmed by BiFc tests (Fig. 3C), including competition analysis (Fig. 3A). Moreover, NS1 can efficiently interact with RIG-I from duck, mouse, and swine (Fig. 3C). Thus, it is possible that NS1 may compete with RNP subunits to bind RIG-I or inhibit the associations between RNP subunits and RIG-I. To address this issue, different RNP subunit- and RIG-I-expressing plasmids were cotransfected into 293T cells along with NS1-encoding plasmid [pCAGGS-WFNS1(ΔS)] or an empty vector (pCAGGS). Interestingly, the expression of WF10-NS1(ΔS) did not interfere with the binding of RNP subunits to RIG-I and in fact appeared to promote BiFc signals (Fig. 3D). This effect was particularly noticeable in cells coexpressing the chimeric RIG-I and chimeric PB2, PB1, or PA constructs, whereas no obvious effects were seen with the chimeric NP (Fig. 3D). Quantitative analysis indicated than overexpression of NS1 led to ~4- to 5-fold increases in average BiFc signal intensity in cells cotransfected with PB2/HRIG, PB1/HRIG, and PA/HRIG plasmids but not in cells cotransfected with NP/HRIG plasmids (data not shown). Several lines of evidence indicate that NS1 can selectively increase viral mRNA synthesis, resulting in preferential viral protein synthesis (49–51). To test whether increased BiFc signals were the result of NS1 stimulation of RNP subunit synthesis, Western blot analysis was performed from cells transfected with plasmids encoding the RNP subunits in the presence or absence of the WF10-NS1(ΔS) expression plasmid. Interestingly, WF10-NS1(ΔS) coexpression did not result in a significant increase in the expression of PB2-NYFP, PB1-NYFP, PA-NYFP, or NP-NCe (Fig. 3E). In a separate study, however, the NS1 from the 2009 pandemic H1N1 virus did promote expression of RNP subunits (data not shown). Therefore, we cannot completely exclude a role for NS1 in the modulation of BiFc signals. Nevertheless, the data clearly show that NS1 coexpression does not negatively affect the interaction of RIG-I with the RNP subunits. The underlying mechanisms for the increase in fluorescence intensities between the RNA polymerase subunits with RIG-I in the presence of WF10 NS1 remain to be determined.

Analysis of association of RNP subunits with RIG-I by confocal microscopy. To further validate the association of RNP subunits with RIG-I, confocal microscopy was employed, revealing the colocalization of different RNP subunits and RIG-I in 293T cells (Fig. 4A). Coexpression PB1 or PA with RIG-I generated overlapped fluorescence signals in the cytoplasm, while coexpression of either PB2 or NP resulted in RIG-I relocalization to the nuclear compartment (Fig. 4A).

Interactions between RNP subunits and RIG-I during virus infection. Next the relationship among RNP subunits and RIG-I during virus infection was investigated. 293T cells were transfected with RIG-I or GFP expression constructs, followed by infection with wild-type WF10 virus. PB2, PB1, PA, and NP could be easily detected in WF10 virus-infected cells but not in mock-infected cells (Fig. 4B). In addition, RIG-I and GFP were expressed and successfully captured by protein G beads coupled with the appropriate antibodies, and RIG-I pulldown, but not GFP pulldown, resulted in cocapture of PB2, PB1, PA, and NP (Fig. 4B). These data provided further evidence for the binding of each RNP subunit with RIG-I during influenza A virus infection.

FIG 3 BiFc competition analysis and effect of NS1 on BiFc signals. (A) BiFc competition analysis. 293T cells growing in 24-well plates were transfected with 0.75 μg of RNP plasmid (pDPPB2-NYFP, pDPPB1-NYFP, pDPPA-NYFP, or pDPNP-Nce) or NS1 plasmid [pc-NS1(ΔS)-NYFP], 0.25 μg of pc-HRIG-CYFP plasmid, and 0.5 μg of pflag-HRIG or pCAGGS-GST plasmid. The cells were incubated for 24 h at 37°C and for 14 h at 30°C prior to staining with rabbit anti-Flag antibody (1:300) or goat anti-GST antibody (1:250) and Alexa Fluor 594-conjugated goat anti-rabbit antibody (1:300) or Alexa Fluor 594-conjugated donkey anti-goat antibody (1:300). The fluorescent signals were captured by a Zeiss SM510 confocal microscope after counterstaining with DAPI. (B) Total BiFc signals from three random fields (about 500 to 600 cells) were collected and determined by ImageJ software and normalized by the cell numbers. The average signal intensity in each control group (GST group) was set as 1, and the percentages of experimental groups (Flag-HRIG groups) relative to the control group are shown. (C) Interaction between NS1 from WF10 virus and RIG-I from various hosts. 293T cells were transfected with WFNS1(ΔS)-NYFP-expressing plasmid together with plasmids encoding CYFP-tagged RIG-I from human, duck, mouse, or swine. After 24 h of incubation at 37°C and 14 h of incubation at 30°C, cells were stained with DAPI and visualized under a confocal microscope. (D) BiFc signals in the absence [(−)] or presence [(+)] of NS1 protein. pDP-based PB2-, PB1-, PA-, and NP-expressing plasmids were cotransfected with pcDNA-based RIG-I-expressing plasmids into 293T cells in combination with an empty pCAGGS vector or pCAGGS-WFNS1(ΔS) plasmid. BiFc signals were viewed at 38 hpt (24 h at 37°C and 14 h at 30°C). (E) Effect of NS1 protein on the expression of viral RNP subunits. Plasmid pDPPB2-NYFP, pDPPB1-NYFP, pDPPA-NYFP, or pDPNP-NCe was cotransfected into 293T cells in parallel with pCAGGS vector or pCAGGS-WFNS1(ΔS) plasmid. Western blots were performed at 36 h posttransfection using antibodies against PB2, PB1, PA, NP, NS1, or GAPDH as indicated in Materials and Methods.

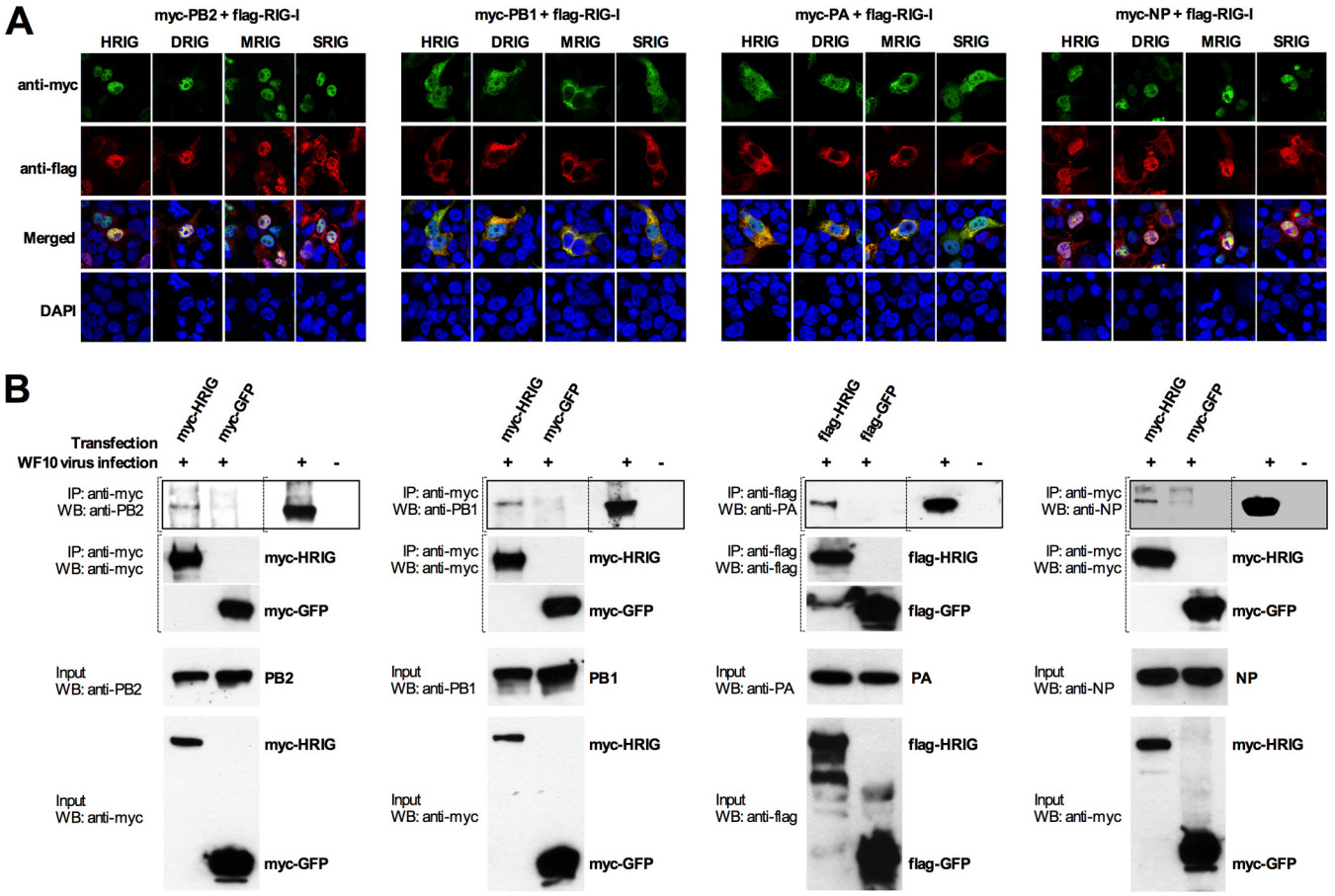

FIG 4 (A) Colocalization of influenza A virus RNP subunits with RIG-I from various hosts. Different combinations of plasmids were cotransfected into 293T cells. At 24 hpt, cells were fixed with 4% paraformaldehyde, permeabilized with 0.2% Triton X-100, and incubated with rabbit anti-Flag antibody and mouse anti-myc antibody, followed by immunostaining with Alexa Fluor 568-labeled donkey anti-rabbit antibody and Alexa Fluor 488-conjugated donkey anti-mouse antibody. Nuclei were counterstained with DAPI. Confocal microscopy was used to examine the localization of Flag-tagged RIG-I (red) and myc-tagged proteins (PB2, PB1, PA, or NP) (green). Merged fields show colocalization of Flag and myc chimeric proteins (yellow). (B) Interaction between RNP subunits and RIG-I during WF10 virus infection. 293T cells were transfected with either pmyc-HRIG or pmyc-GFP (where indicated, pflag-HRIG and pflag-GFP were used instead). At 32 hpt, cells were infected with WF10 virus (MOI = 2) for 14 h and lysed with NP-40 buffer. Anti-myc (or anti-Flag) antibody was subsequently used to precipitate immune complexes containing myc-HRIG (or Flag-HRIG). Western blotting was conducted using antibodies recognizing PB2, PB1, PA, or NP (top WB images).

Exogenous expression of either PB2 or NP or virus infection induces partial nuclear accumulation of endogenous RIG-I. Some cytoplasmic proteins, such as HSP90 (35), HSP70 (52, 53), or p23 (54), were reported previously to relocalize to the nucleus via their interactions with viral RNA polymerase. The nuclear import of exogenously expressed RIG-I by PB2 or NP was also found in the BiFc and confocal analysis. To elucidate whether this is also the case for endogenous RIG-I (endo-RIG-I), the subcellular location of endo-RIG-I was examined in A549 cells transiently transfected with myc-tagged PB2 or NP. Contrary to the almost exclusively cytoplasmic distribution of RIG-I in empty vector-transfected cells, the nuclear translocation of endo-RIG-I was clearly observed in cells expressing myc-PB2 or myc-NP. Approximately 12% to 18% of cells showed nuclear localization of RIG-I, whereas 9% or 7% of cells displayed both nuclear and cytoplasmic localization of RIG-I (Fig. 5A and C). Noticeably, fluorescence labeling of myc-PB2 or myc-NP exhibited overlapped signals with endo-RIG-I, suggesting their interactions in A549 cells (Fig. 5A). The subcellular distribution pattern of endo-RIG-I was also examined in the context of WF10 virus-infected cells. The location of PB2, PB1, and PA during virus infection was not analyzed because the antibodies were unsuitable for immunofluorescence assay (IFA). An NS1-deleted WF10 virus was also constructed to determine whether RIG-I relocalization is at least partially modulated by the RNP subunits. The NS1 deletion was confirmed by sequencing and failure to express NS1 in Western blot analysis (Fig. 5D). Enhanced RIG-I expression was observed in A549 cells infected with either wild-type or NS1-deleted WF10 virus (Fig. 5B and F), which corresponds with previous reports regarding upregulated RIG-I expression by influenza virus (46, 55, 56). In addition, compared with mock-infected cells, both viruses elicited the nuclear import of endo-RIG-I (Fig. 5B, lower half, and Fig. 5C, bottom right graph), suggesting that virus components (perhaps RNPs) other than NS1 are in part responsible for its translocation. Colocalization of NP and RIG-I within nuclei in the enlarged images (Fig. 5B, upper half) further strengthens the case for an association between RNPs and endo-RIG-I.

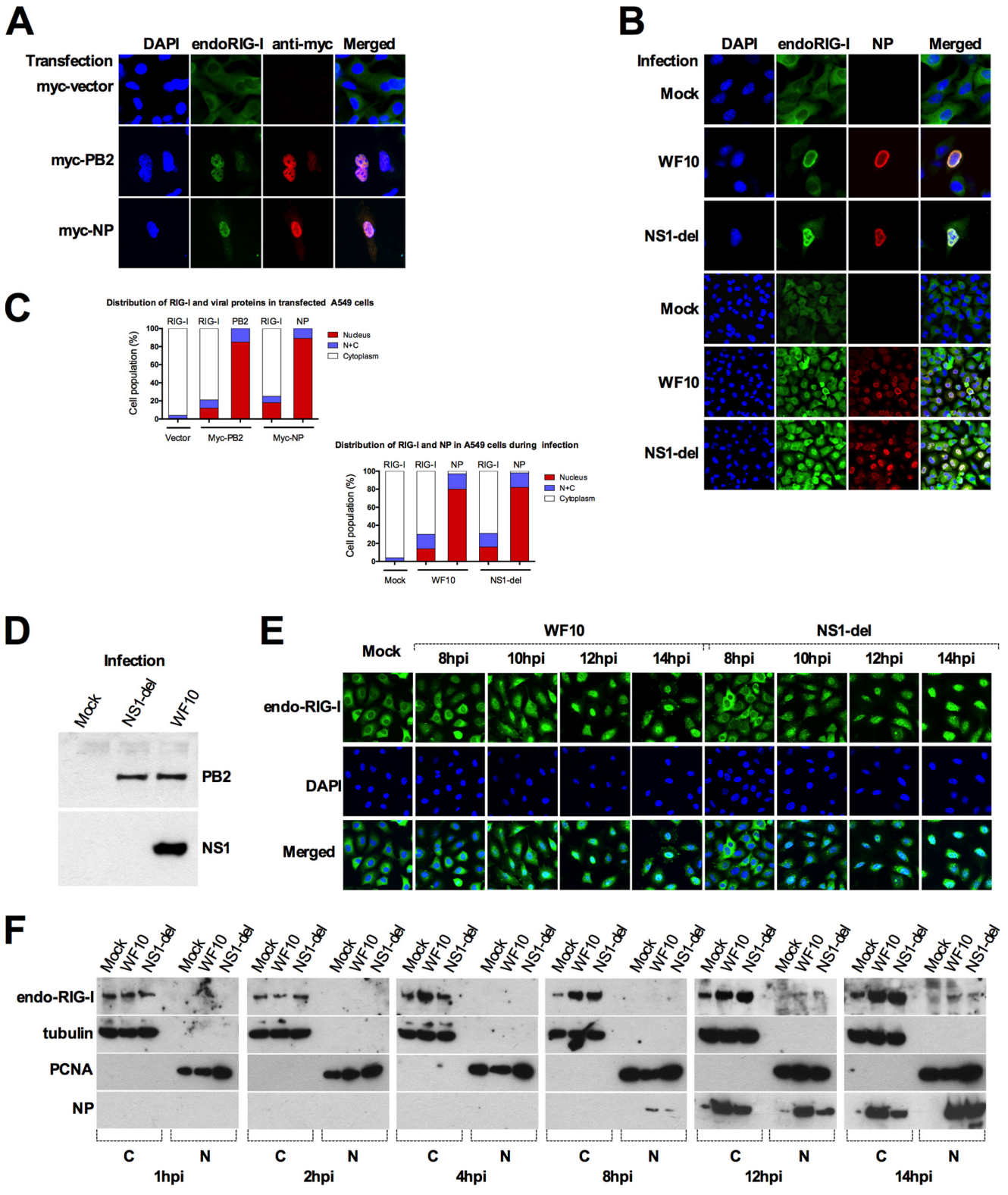

FIG 5 (A) Relocalization of endo-RIG-I in A549 cells during transfection with PB2- or NP-expressing plasmids. The myc-tagged PB2 or NP constructs or pmyc vector was delivered into A549 cells. At 24 hpt, RIG-I was detected with rabbit anti-RIG-I antibody and Alexa Fluor 488-conjugated donkey anti-rabbit antibody, while myc-PB2 or myc-NP was probed with mouse anti-myc antibody and Alexa Fluor 568-conjugated donkey anti-mouse antibody. (B) Subcellular localization of RIG-I and NP in virus-infected cells. After 14 h of infection of A549 cells with wild-type or NS1-deleted WF10 virus (MOI = 5), the cells were fixed and stained with rabbit anti-RIG-I and mouse anti-NP antibodies. The power of magnification is ×600, with enlarged fields shown in the top three rows. (C) Quantitation analysis of the percentage of cell populations based on the intracellular distribution pattern of RIG-I versus myc-PB2 or myc-NP (top left graph) or NP (bottom right graph) in virus-infected cells. (D) Confirmation of NS1-deleted virus by Western blotting. MDCK cells were infected with wild-type (MOI = 0.1) or NS1-deleted (MOI = 2) WF10 virus. At 16 hpi, Western blotting was conducted using NS1 or PB2 antibody. (E and F) Intracellular distribution of endo-RIG-I at different times postinfection. A549 cells were infected (MOI = 5) with wild-type or NS1-deleted WF10 virus. At the indicated time points, cells were fixed and subjected to IFA analysis using RIG-I antibody, while the cytoplasmic (C) or nuclear (N) fractions were isolated and subjected to WB analysis using antibodies against RIG-I, tubulin, PCNA, and viral NP. Tubulin and PCNA serve as cytoplasmic and nuclear protein markers, respectively.

Partial relocalization of RIG-I into the nucleus at late stages of infection. In order to investigate the translocation kinetics of endo-RIG-I in the infection process, A549 cells were infected with wild-type or NS1-deleted WF10 virus (MOI = 5). At different times postinfection (1, 2, 4, 6, 8, 10, 12, and 14 hpi), the localization of endo-RIG-I was examined (Fig. 5E). In agreement with previous studies (46, 55, 56), the levels of endo-RIG-I increased significantly in cells infected with either virus (Fig. 5F). In addition, endo-RIG-I was almost solely found in the cytoplasmic fractions in control cells and virus-infected cells prior to 8 hpi (Fig. 5E and F). Then it started to move partially toward the nucleus. At later time points (e.g., 12 or 14 hpi), a proportion of endo-RIG-I was found in the nucleus (Fig. 5E and F) or an area surrounding the nucleus (Fig. 5E), indicating that the nuclear import of endo-RIG-I is induced by the virus and that it is a late event and can occur in the presence or absence of NS1. Interestingly, a minor proportion of endo-RIG-I was located on the plasma membrane ruffle and formed a "hedgehog-like" shape at late infection phase (e.g., WF10 virus-infected cells at 14 hpi in Fig. 5E), presumably caused by the surface bleb of apoptotic cells during virus infection (57–59).

Effects of RNP subunits on the activation of IFN-β or ISRE activity by RIG-I. Interaction of NS1 with RIG-I, TRIM25α, or Riplet antagonizes IFN production and negatively modulates the host's antiviral defense (16, 22, 47). Furthermore, PB1-F2 interferes with IFN induction via MAVS (26, 27). The association between RNP subunits and RIG-I may also play a previously undefined role in interferon signaling. Therefore, IFN-β promoter-driven luciferase reporter gene assays were performed to determine whether RNP subunits of influenza virus affect the generation of IFN triggered by RIG-I. 293T cells were transfected with a plasmid expressing Flag-tagged human RIG-I (Flag-HRIG) along with various amounts of PB2-, PB1-, PA- NP-, and NS1-expressing plasmids for 24 h and then stimulated with 5′ppp RNA (a strict RIG-I-specific ligand containing 19-mer double-stranded RNA with a 5′ triphosphate) to induce IFN synthesis. Combined treatment of 293T cells with RIG-I and 5′ppp RNA resulted in a marked increase in IFN-β promoter induction (49.7-fold) compared with that in the mock-treated cells (Fig. 6A). In the positive-control group, NS1 from WF10 virus exhibited dramatic inhibition of the IFN-β promoter (74% reduction) even at a low transfection dose (0.24 μg). However, PB2, PB1, or PA alone only slightly decreased IFN-β promoter activity, by about 36 to ~40% at a high transfection dose (1.2 μg). NP did not show statistically significant repression. Only mild (and even negligible) inhibition was observed if the mixtures of two components (PB2 and PB1) or the RNA polymerase complex (PB2, PB1, and PA) or the vRNP complex (polymerase complex plus NP) were coexpressed with RIG-I and later stimulated by 5′ppp RNA (Fig. 6A). Results from another reporter assay using interferon-stimulated response element (ISRE) were even less prominent, with only suppression by NS1 at a high transfection dose having statistical significance. These results suggest a yet-to-be-defined biological role (if any) for the interaction of RNP subunits with RIG-I.

Examination of IFN induction using quantitative RT-PCR and IRF3 phosphorylation assay. To further clarify the role of RNP subunits in IFN activation and IFN signaling transduction, the impact of each individual RNP subunit on mRNA levels of human IFN-β was analyzed. To stimulate IFN, different inducers were employed after 24 h of transfection of 293T cells with Flag-HRIG plasmid or empty Flag vector. Either the specific RIG-I binding ligand (5′ppp RNA) or RNA from WF10 virus-infected or uninfected Vero cells was used as an IFN inducer (Fig. 6C and D), essentially as described previously (60, 61). As expected, IFN-β mRNA levels were substantially elevated by the coadministration of RIG-I and either 5′ppp RNA or viral RNA (VR) but not with control cellular RNA (CR). Moreover, IFN-β mRNA decreased to 7.9% (Fig. 6C, 5′ppp RNA) or 32.0% (Fig. 6D, VR) compared to the levels for controls in cells expressing NS1. In contrast, PB2, PB1, and PA did not repress IFN-β activation (Fig. 6C and D). Interestingly, NP upregulated IFN-β mRNA levels, the significance of which remains to be determined.

IRF3 is known to be an important adaptor of the RIG-I signaling pathway. The phosphorylation of IRF3 and the subsequent nuclear import of IRF3 play vital roles in IFN activation (62). Taking this into consideration, it was examined whether individually expressed RNP subunits have an effect on levels of IRF3 phosphorylation (via the monitoring of phosphorylated Ser396 [p-IRF3] and total IRF3 [IRF3]). Quantitative analysis for the intensities of protein bands in Western blots showed that the ratio of p-IRF3 to IRF3 remained unchanged upon the overexpression of each RNP subunit compared to the vector-alone control (Fig. 7). In contrast and as expected, the p-IRF3/IRF3 ratio was markedly decreased by expression of NS1 compared to that with the negative control (Fig. 7).

DISCUSSION

Interactions between viral proteins and host factors govern the adaptation and pathogenicity of viruses in different hosts. In this regard, the influenza virus RNP complex plays a vital role (6, 63, 64). Influenza virus polymerase complex subunits PB2, PB1, PA, and NP can interact, alone or in combination, with a multitude of host factors involved in various intracellular events such as cellular transcription, nuclear-cytoplasmic transport, protein subcellular trafficking, and the host immune response (6, 64, 65). However, the exact mechanisms that modulate vRNP-host factor interactions and the outcome of infection remain largely elusive.

In this study, the associations of influenza A virus RNP subunits with RIG-I were analyzed using different approaches. Co-IP tests showed the RNA-independent interactions of each viral RNA polymerase subunit (PB2, PB1, and PA) with RIG-I and RNA-dependent interaction of NP with RIG-I (Fig. 1). In BiFc analysis, expression of either PB2, PB1, PA, or NP chimeric constructs harboring a split fluorescence protein sequence interacted with chimeric RIG-I protein fused to a complementary split fluorescence protein, resulting in bright fluorescence signals in 293T cells (Fig. 2). Interestingly, the BiFc signals emitted by PB1-RIG-I or PA-RIG-I interactions were predominantly distributed in the cytoplasm, whereas the signals produced by PB2-RIG-I or NP-RIG-I interactions occurred mainly in the nuclei. Similar results were obtained in confocal analysis (Fig. 4A). These findings are compatible with the previous reports on the major subcellular localization of individual RNP subunits in cells (35, 37–39). Finally, co-IP results from infection experiments (Fig. 4B) provided further evidence for RIG-I binding to each of the RNP components.

The NS1 proteins from various influenza virus strains have been shown to differentially interact with TRIM25α (an important regulator of RIG-I) from different species (16). Human TRIM25 was shown to bind NS1 proteins from human, swine, or avian viruses, whereas mouse TRIM25 did not (16), suggesting

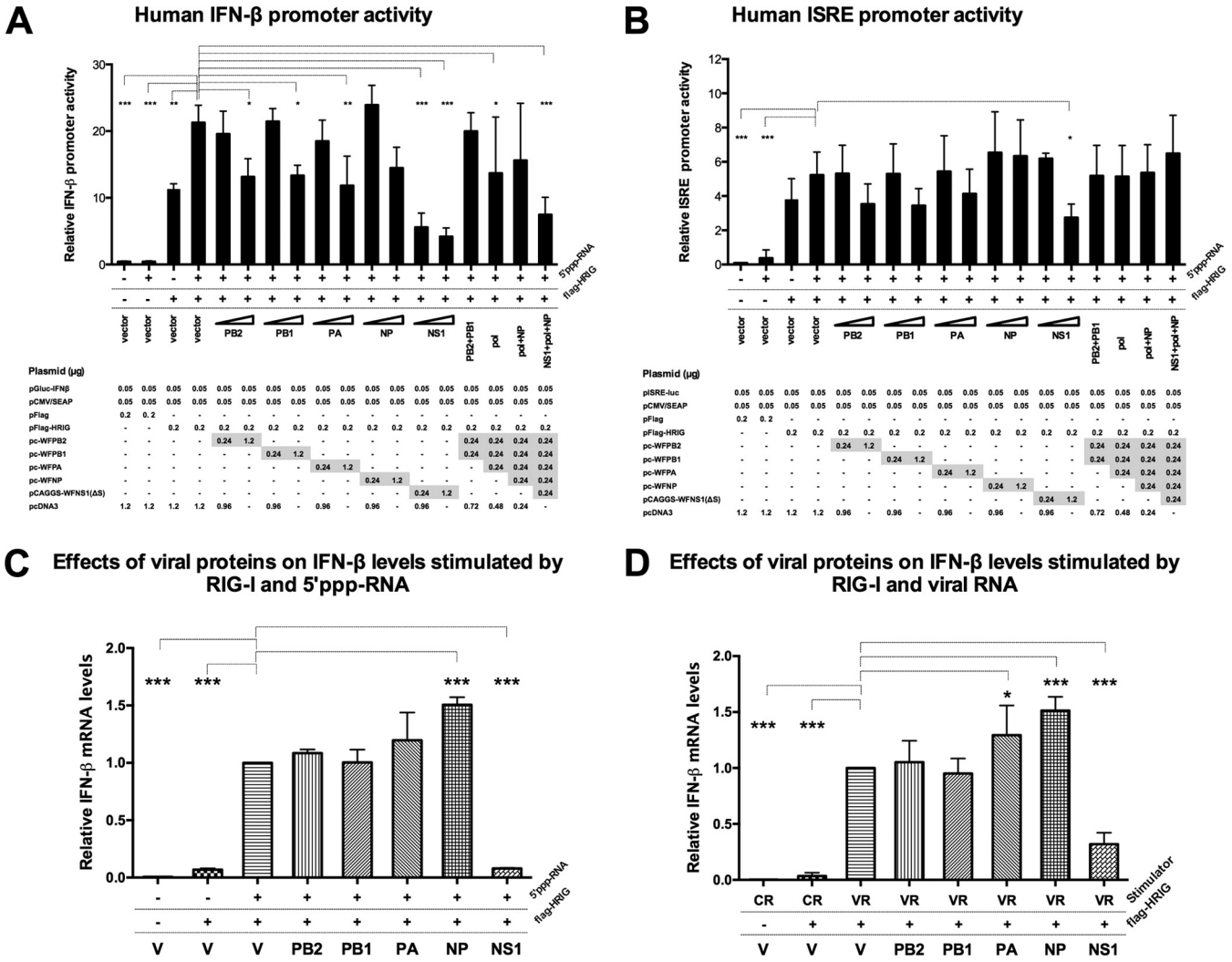

FIG 6 Effects of viral RNP components on the IFN induction by RIG-I in reporter and qRT-PCR assays. (A) Dose-dependent and combined effects of RNP components on IFN-β promoter activation by RIG-I and 5′ppp RNA. Expression plasmids for PB2, PB1, PA, NP, or NS1 were transfected into 293T cells in 24-well plates, either alone (0.24 μg or 1.2 μg) or in combination (0.24 μg for each plasmid), together with Flag-HRIG plasmid (0.2 μg), pGluc-IFNβ construct (0.05 μg), and pCMV/SEAP plasmid (0.05 μg). Empty pcDNA3 vector was added when necessary to keep the total DNA amount constant in each group. 5′ppp RNA (0.5 μg/well) was delivered into cells by Lipofectamine 2000 at 24 hpt. *Gaussia* luciferase (Gluc) and secreted alkaline phosphatase (SEAP) activities in supernatants were measured at 24 h of stimulation of 5′ppp RNA. The relative IFN-β promoter activity was expressed as the ratio of Gluc to SEAP. Data are presented as means ± standard deviations of samples from three independent experiments. Values from each group were compared to those of the control group transfected with empty vector but stimulated by 5′ppp RNA. (B) ISRE activation by RIG-I and 5′ppp RNA in the presence or absence of viral RNP components. Reporter assays were performed as described above, except that the plasmid pGluc-IFNβ was replaced by pISRE-Luc. (C and D) Examination of IFN-β mRNA abundance in the presence or absence of viral proteins. 293T cells in a 24-well plate were transfected with 1.3 μg of expression plasmids for PB2, PB1, PA, NP, or NS1 or empty vector (V) as well as 0.2 μg of pflag-HRIG plasmid for 24 h. The cells were further transfected with either 1 μg of 5′ppp RNA or 1 μg of RNA from influenza virus-infected Vero cells (VR) or uninfected Vero cells (CR) for 11 h. RNAs were extracted and qRT-PCR was performed using SYBR green I and primers specific for IFN-β and β-actin. The data represent the results of three independent experiments with 3 replicates per experiment. The relative mRNA levels of IFN-β were measured as a ratio of IFN-β to β-actin using the $2^{-\Delta\Delta CT}$ method. The *P* values, when significant (*, $P < 0.05$; **, $P < 0.01$; ***, $P < 0.001$) by one-way ANOVA, are shown above the bars.

species-specific differences of the TRIM25 interaction with NS1 that might influence the pathogenesis of influenza in different hosts. Unlike the TRIM25-NS1 interaction, RIG-I interactions with RNP subunits were not species specific, despite significant amino acid differences between RIG-I from birds (duck) and mammals (human, swine, and mouse), suggesting a conserved property of RIG-I.

Previous studies found that the associations between viral RNA polymerase and cytoplasmic proteins such as HSP90 (35), HSP70 (52, 53), or P23 (54) led to the relocalization of the latter into the nucleus. In the present study, a small proportion of endogenous RIG-I also translocated into the nuclei of cells overexpressing PB2 or NP or cells infected with wild-type or NS1-deleted WF10 virus (Fig. 5). In addition, the nuclear translocation of RIG-I is a late event during virus infection and independent of the expression of NS1 (Fig. 5). It is tempting to speculate that interactions of RNP subunits with RIG-I are involved in this process.

To facilitate virus replication, RNP subunits of influenza A

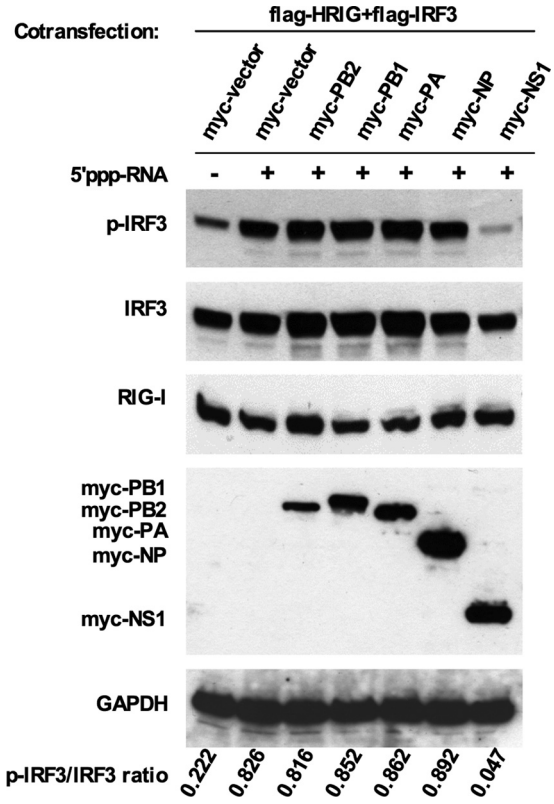

FIG 7 Effects of viral proteins on phosphorylation of IRF3. Myc-tagged constructs encoding PB2, PB1, PA, NP, or NS1 from WF10 virus (2 μg) or pmyc empty vector (2 μg) were transfected into 293T cells (12-well plate) along with 0.3 μg of pflag-HRIG plasmid and 0.7 μg of pflag-IRF3 plasmid. Twenty-four hours later, cells were further transfected with 5′ppp RNA for 12 h. The cells were subsequently lysed and subjected to Western blot analysis using antibodies specific for phospho-IRF3 (Ser396), IRF3, RIG-I, myc tag, and GAPDH. The band intensities of p-IRF3 (phosphorylated IRF3) and IRF3 (total IRF3) were calculated by ImageJ software, and the ratios of p-IRF3 to IRF3 are shown at the bottom.

virus may manipulate IFN signaling transduction via their associations with RIG-I. This effect would complement the activities of some other influenza virus proteins that have already been reported to affect the RIG-I signaling pathway at different steps (66). In addition, NS1 can directly target and inhibit RIG-I (9, 10, 22), TRIM25α (22), or Riplet (16); PB1-F2 acts on MAVS, hence blocking IFN production (25–27). More recently, overexpression of PB2 (25, 28, 30), PB1 (25, 30), or PA (25, 30) from human virus strains (PR8 or WSN) was found to repress IFN-β promoter-driven reporter activity via interactions with MAVS. In addition, a high-throughput screening for the interacting partners of influenza virus in human cells illustrated physical associations among RNP subunits and a variety of regulators of interferon response (67). In this regard, the results presented here are in partial agreement with the above-mentioned studies, as PB2, PB1, or PA from WF10 virus (an avian virus) individually reduced the activation of IFN-β promoter in reporter assays (Fig. 6A and B). However, the RNA polymerase-mediated IFN-inhibiting effect is mild and had no effect on IFN-β mRNA levels (Fig. 6C and D) or IRF3 phosphorylation (Fig. 7). Altogether, the RNA polymerase subunits from the WF10 virus do not have a significant impact on IFN activation elicited by RIG-I in human cells *in vitro*. It remains to be determined if these interactions have any significant role *in vivo*.

Interestingly, NP neither suppressed the activation of the IFN-β promoter or ISRE (Fig. 6A and B) nor decreased the phosphorylation of IRF3 (Fig. 7). On the contrary, qRT-PCR assays suggest that NP upregulated IFN mRNA levels (Fig. 6C and D). Previous studies have shown that influenza virus vRNA wraps around the NP, being exposed to the surface and, thus, accessible to RIG-I (68, 69).

It was presumed that interactions of RNP subunits with RIG-I could have special significance for the early phase of influenza A virus infection, when NS1 has yet to be synthesized. In addition, the incoming viral RNA is encapsidated with NP and the 5′ppp dsRNA panhandle structure is bound by the viral polymerase. Little is known about how the host cell senses the invading viral genome and triggers innate immune responses and how viruses counteract the immune recognition during this time. Using Rift Valley fever virus (RVFV) and La Crosse virus (LACV), two members of *Bunyaviridae* family that possess 5′ppp dsRNA panhandle structures in their negative-stranded genome RNA similar to that in influenza A virus, Weber et al. showed that the interaction between RIG-I and viral nucleocapsids (including both viral nucleoprotein and the 5′ppp dsRNA structure) is necessary for the initiation of innate immunity (70). In our study, although RNA polymerase components PB2, PB1, and PA were shown to directly associate with RIG-I, no significant effects on IFN production were observed. It is conceivable to speculate, then, that the viral RNA polymerase would not prevent access of RIG-I to the viral 5′ppp dsRNA structure and the subsequent activation of IFN. Furthermore, it should be noted that the WF10 virus used in this study belongs to the H9N2 subtype of viruses, responsible for donating their internal genes to the highly pathogenic H5N1 virus (71), the novel H7N9 virus (72), and the newly identified H10N8 virus that crossed to humans (73). However, in view that WF10 is still a typical avian influenza virus, the possibility that RNA polymerase complexes from avian influenza viruses do not efficiently exert IFN-antagonizing ability in human cells cannot be completely excluded.

Another possible scenario in the outcome of the interactions between RIG-I and RNP components is the direct suppression of viral RNA polymerase activity by RIG-I. RIG-I (also known as DDX58) belongs to the DExD/H helicase family. Some members of this family have been shown to associate with viral RNP components and affect the polymerase activity. For instance, the associations of DDX3 (74), DDX5 (74, 75), and DDX17 (75, 76) with viral polymerase or NP have been identified, and DDX5 (76) and DDX17 (76) were found to facilitate viral RNA synthesis. In addition, DDX39B (UAP56) (77, 78) and its paralog DDX39 (URH39) (78) interact with NP, and DDX39B helps virus replication via promoting the formation of the NP-RNA complex or preventing the formation of dsRNA and the subsequent activation of innate immune response (78). Conversely, DDX21 restricts influenza virus by binding PB1 and decreasing the assembly of viral polymerase (79). Our unpublished data from reporter assays also showed that overexpression of RIG-I markedly suppressed virus polymerase activity in 293T cells, but the suppression could be attributed to IFN or other inflammatory cytokines elicited by RIG-I activation. Previous studies indicated that a single mutation in residue 183 (S183I) (80) or residue 55 (T55I) (81, 82) of RIG-I completely eliminated its ability to transduce signal and trigger the innate immune response. If these two RIG-I mutants still maintain the capacity to interact with vRNP components, they can serve as

useful tools to investigate the direct effect of RIG-I on viral polymerase activity in RIG-I knockout mouse embryo fibroblasts. A detailed analysis of the relationship of RIG-I mutants with vRNP and their effects on virus replication will be undertaken in the future.

In conclusion, this study highlights the direct association of influenza virus RNP subunits with RIG-I from various species. These interactions, however, seemed to be unrelated to the modulation of the IFN signaling pathway. The significance of RNP subunits in modulating immune responses and virulence of influenza A virus *in vivo* deserves further attention.

ACKNOWLEDGMENTS

We thank Andrea Ferrero, Johanna Lavigne, and Qiong Chen for their laboratory managerial skills and assistance.

D.R.P. and W.L. conceived and designed the experiments. W.L., H.C., and A.O. performed the experiments. W.L., T.S., and D.R.P. analyzed the data and prepared the manuscript. H.C. and T.S. contributed reagents, materials, and analysis tools.

This research was funded by NIAID/NIH contract HHSN 26620070001.

REFERENCES

1. **Guilligay D, Tarendeau F, Resa-Infante P, Coloma R, Crepin T, Sehr P, Lewis J, Ruigrok RW, Ortin J, Hart DJ, Cusack S.** 2008. The structural basis for cap binding by influenza virus polymerase subunit PB2. Nat. Struct. Mol. Biol. **15:**500–506. http://dx.doi.org/10.1038/nsmb.1421.
2. **Fodor E, Crow M, Mingay LJ, Deng T, Sharps J, Fechter P, Brownlee GG.** 2002. A single amino acid mutation in the PA subunit of the influenza virus RNA polymerase inhibits endonucleolytic cleavage of capped RNAs. J. Virol. **76:**8989–9001. http://dx.doi.org/10.1128/JVI.76.18.8989-9001.2002.
3. **Biswas SK, Nayak DP.** 1994. Mutational analysis of the conserved motifs of influenza A virus polymerase basic protein 1. J. Virol. **68:**1819–1826.
4. **Portela A, Digard P.** 2002. The influenza virus nucleoprotein: a multifunctional RNA-binding protein pivotal to virus replication. J. Gen. Virol. **83:**723–734.
5. **Cros JF, Palese P.** 2003. Trafficking of viral genomic RNA into and out of the nucleus: influenza, Thogoto and Borna disease viruses. Virus Res. **95:**3–12. http://dx.doi.org/10.1016/S0168-1702(03)00159-X.
6. **Naffakh N, Tomoiu A, Rameix-Welti MA, van der Werf S.** 2008. Host restriction of avian influenza viruses at the level of the ribonucleoproteins. Annu. Rev. Microbiol. **62:**403–424. http://dx.doi.org/10.1146/annurev.micro.62.081307.162746.
7. **Kato H, Takeuchi O, Sato S, Yoneyama M, Yamamoto M, Matsui K, Uematsu S, Jung A, Kawai T, Ishii KJ, Yamaguchi O, Otsu K, Tsujimura T, Koh CS, Reis e Sousa C, Matsuura Y, Fujita T, Akira S.** 2006. Differential roles of MDA5 and RIG-I helicases in the recognition of RNA viruses. Nature **441:**101–105. http://dx.doi.org/10.1038/nature04734.
8. **Loo YM, Fornek J, Crochet N, Bajwa G, Perwitasari O, Martinez-Sobrido L, Akira S, Gill MA, Garcia-Sastre A, Katze MG, Gale M, Jr.** 2008. Distinct RIG-I and MDA5 signaling by RNA viruses in innate immunity. J. Virol. **82:**335–345. http://dx.doi.org/10.1128/JVI.01080-07.
9. **Pichlmair A, Schulz O, Tan CP, Naslund TI, Liljestrom P, Weber F, Reis e Sousa C.** 2006. RIG-I-mediated antiviral responses to single-stranded RNA bearing 5′-phosphates. Science **314:**997–1001. http://dx.doi.org/10.1126/science.1132998.
10. **Rehwinkel J, Tan CP, Goubau D, Schulz O, Pichlmair A, Bier K, Robb N, Vreede F, Barclay W, Fodor E, Reis e Sousa C.** 2010. RIG-I detects viral genomic RNA during negative-strand RNA virus infection. Cell **140:**397–408. http://dx.doi.org/10.1016/j.cell.2010.01.020.
11. **Kato H, Takeuchi O, Mikamo-Satoh E, Hirai R, Kawai T, Matsushita K, Hiiragi A, Dermody TS, Fujita T, Akira S.** 2008. Length-dependent recognition of double-stranded ribonucleic acids by retinoic acid-inducible gene-I and melanoma differentiation-associated gene 5. J. Exp. Med. **205:**1601–1610. http://dx.doi.org/10.1084/jem.20080091.
12. **Baum A, Sachidanandam R, Garcia-Sastre A.** 2010. Preference of RIG-I for short viral RNA molecules in infected cells revealed by next-generation sequencing. Proc. Natl. Acad. Sci. U. S. A. **107:**16303–16308. http://dx.doi.org/10.1073/pnas.1005077107.
13. **West AP, Shadel GS, Ghosh S.** 2011. Mitochondria in innate immune responses. Nat. Rev. Immunol. **11:**389–402. http://dx.doi.org/10.1038/nri2975.
14. **Edwards MR, Slater L, Johnston SL.** 2007. Signalling pathways mediating type I interferon gene expression. Microbes Infect. **9:**1245–1251. http://dx.doi.org/10.1016/j.micinf.2007.06.008.
15. **Schoggins JW, Wilson SJ, Panis M, Murphy MY, Jones CT, Bieniasz P, Rice CM.** 2011. A diverse range of gene products are effectors of the type I interferon antiviral response. Nature **472:**481–485. http://dx.doi.org/10.1038/nature09907.
16. **Rajsbaum R, Albrecht RA, Wang MK, Maharaj NP, Versteeg GA, Nistal-Villan E, Garcia-Sastre A, Gack MU.** 2012. Species-specific inhibition of RIG-I ubiquitination and IFN induction by the influenza A virus NS1 protein. PLoS Pathog. **8:**e1003059. http://dx.doi.org/10.1371/journal.ppat.1003059.
17. **Zou J, Chang M, Nie P, Secombes CJ.** 2009. Origin and evolution of the RIG-I like RNA helicase gene family. BMC Evol. Biol. **9:**85. http://dx.doi.org/10.1186/1471-2148-9-85.
18. **Barber MR, Aldridge JR, Jr, Webster RG, Magor KE.** 2010. Association of RIG-I with innate immunity of ducks to influenza. Proc. Natl. Acad. Sci. U. S. A. **107:**5913–5918. http://dx.doi.org/10.1073/pnas.1001755107.
19. **Karpala AJ, Stewart C, McKay J, Lowenthal JW, Bean AG.** 2011. Characterization of chicken Mda5 activity: regulation of IFN-beta in the absence of RIG-I functionality. J. Immunol. **186:**5397–5405. http://dx.doi.org/10.4049/jimmunol.1003712.
20. **Hale BG, Randall RE, Ortin J, Jackson D.** 2008. The multifunctional NS1 protein of influenza A viruses. J. Gen. Virol. **89:**2359–2376. http://dx.doi.org/10.1099/vir.0.2008/004606-0.
21. **Talon J, Horvath CM, Polley R, Basler CF, Muster T, Palese P, Garcia-Sastre A.** 2000. Activation of interferon regulatory factor 3 is inhibited by the influenza A virus NS1 protein. J. Virol. **74:**7989–7996. http://dx.doi.org/10.1128/JVI.74.17.7989-7996.2000.
22. **Gack MU, Albrecht RA, Urano T, Inn KS, Huang IC, Carnero E, Farzan M, Inoue S, Jung JU, Garcia-Sastre A.** 2009. Influenza A virus NS1 targets the ubiquitin ligase TRIM25 to evade recognition by the host viral RNA sensor RIG-I. Cell Host Microbe **5:**439–449. http://dx.doi.org/10.1016/j.chom.2009.04.006.
23. **Kochs G, Garcia-Sastre A, Martinez-Sobrido L.** 2007. Multiple anti-interferon actions of the influenza A virus NS1 protein. J. Virol. **81:**7011–7021. http://dx.doi.org/10.1128/JVI.02581-06.
24. **Nemeroff ME, Barabino SM, Li Y, Keller W, Krug RM.** 1998. Influenza virus NS1 protein interacts with the cellular 30 kDa subunit of CPSF and inhibits 3′end formation of cellular pre-mRNAs. Mol. Cell **1:**991–1000. http://dx.doi.org/10.1016/S1097-2765(00)80099-4.
25. **Varga ZT, Grant A, Manicassamy B, Palese P.** 2012. Influenza virus protein PB1-F2 inhibits the induction of type I interferon by binding to MAVS and decreasing mitochondrial membrane potential. J. Virol. **86:**8359–8366. http://dx.doi.org/10.1128/JVI.01122-12.
26. **Varga ZT, Ramos I, Hai R, Schmolke M, Garcia-Sastre A, Fernandez-Sesma A, Palese P.** 2011. The influenza virus protein PB1-F2 inhibits the induction of type I interferon at the level of the MAVS adaptor protein. PLoS Pathog. **7:**e1002067. http://dx.doi.org/10.1371/journal.ppat.1002067.
27. **Dudek SE, Wixler L, Nordhoff C, Nordmann A, Anhlan D, Wixler V, Ludwig S.** 2011. The influenza virus PB1-F2 protein has interferon-antagonistic activity. Biol. Chem. **392:**1135–1144. http://dx.doi.org/10.1515/BC.2011.174.
28. **Graef KM, Vreede FT, Lau YF, McCall AW, Carr SM, Subbarao K, Fodor E.** 2010. The PB2 subunit of the influenza virus RNA polymerase affects virulence by interacting with the mitochondrial antiviral signaling protein and inhibiting expression of beta interferon. J. Virol. **84:**8433–8445. http://dx.doi.org/10.1128/JVI.00879-10.
29. **Patel D, Schultz LW, Umland TC.** 2013. Influenza A polymerase subunit PB2 possesses overlapping binding sites for polymerase subunit PB1 and human MAVS proteins. Virus Res. **172**(1–2):75–80. http://dx.doi.org/10.1016/j.virusres.2012.12.003.
30. **Iwai A, Shiozaki T, Kawai T, Akira S, Kawaoka Y, Takada A, Kida H, Miyazaki T.** 2010. Influenza A virus polymerase inhibits type I interferon induction by binding to interferon beta promoter stimulator 1. J. Biol. Chem. **285:**32064–32074. http://dx.doi.org/10.1074/jbc.M110.112458.
31. **Perez DR, Lim W, Seiler JP, Yi G, Peiris M, Shortridge KF, Webster RG.**

2003. Role of quail in the interspecies transmission of H9 influenza A viruses: molecular changes on HA that correspond to adaptation from ducks to chickens. J. Virol. **77:**3148–3156. http://dx.doi.org/10.1128/JVI.77.5.3148-3156.2003.
32. **Reed LJ, Muench H.** 1938. A simple method for estimating fifty percent endpoints. Am. J. Hyg. **27:**493–497.
33. **Shyu YJ, Liu H, Deng X, Hu CD.** 2006. Identification of new fluorescent protein fragments for bimolecular fluorescence complementation analysis under physiological conditions. Biotechniques **40:**61–66. http://dx.doi.org/10.2144/000112036.
34. **Fodor E, Smith M.** 2004. The PA subunit is required for efficient nuclear accumulation of the PB1 subunit of the influenza A virus RNA polymerase complex. J. Virol. **78:**9144–9153. http://dx.doi.org/10.1128/JVI.78.17.9144-9153.2004.
35. **Naito T, Momose F, Kawaguchi A, Nagata K.** 2007. Involvement of Hsp90 in assembly and nuclear import of influenza virus RNA polymerase subunits. J. Virol. **81:**1339–1349. http://dx.doi.org/10.1128/JVI.01917-06.
36. **Kato H, Takahasi K, Fujita T.** 2011. RIG-I-like receptors: cytoplasmic sensors for non-self RNA. Immunol. Rev. **243:**91–98. http://dx.doi.org/10.1111/j.1600-065X.2011.01052.x.
37. **Deng T, Sharps J, Fodor E, Brownlee GG.** 2005. In vitro assembly of PB2 with a PB1-PA dimer supports a new model of assembly of influenza A virus polymerase subunits into a functional trimeric complex. J. Virol. **79:**8669–8674. http://dx.doi.org/10.1128/JVI.79.13.8669-8674.2005.
38. **Huet S, Avilov SV, Ferbitz L, Daigle N, Cusack S, Ellenberg J.** 2010. Nuclear import and assembly of influenza A virus RNA polymerase studied in live cells by fluorescence cross-correlation spectroscopy. J. Virol. **84:**1254–1264. http://dx.doi.org/10.1128/JVI.01533-09.
39. **Loucaides EM, von Kirchbach JC, Foeglein A, Sharps J, Fodor E, Digard P.** 2009. Nuclear dynamics of influenza A virus ribonucleoproteins revealed by live-cell imaging studies. Virology **394:**154–163. http://dx.doi.org/10.1016/j.virol.2009.08.015.
40. **Ozalp C, Szczesna-Skorupa E, Kemper B.** 2005. Bimolecular fluorescence complementation analysis of cytochrome p450 2c2, 2e1, and NADPH-cytochrome p450 reductase molecular interactions in living cells. Drug Metab. Dispos. **33:**1382–1390. http://dx.doi.org/10.1124/dmd.105.005538.
41. **Shyu YJ, Hu CD.** 2008. Fluorescence complementation: an emerging tool for biological research. Trends Biotechnol. **26:**622–630. http://dx.doi.org/10.1016/j.tibtech.2008.07.006.
42. **Wilson CG, Magliery TJ, Regan L.** 2004. Detecting protein-protein interactions with GFP-fragment reassembly. Nat. Methods **1:**255–262. http://dx.doi.org/10.1038/nmeth1204-255.
43. **Kodama Y, Hu CD.** 2012. Bimolecular fluorescence complementation (BiFC): a 5-year update and future perspectives. Biotechniques **53:**285–298. http://dx.doi.org/10.2144/000113943.
44. **Hudry B, Viala S, Graba Y, Merabet S.** 2011. Visualization of protein interactions in living Drosophila embryos by the bimolecular fluorescence complementation assay. BMC Biol. **9:**5. http://dx.doi.org/10.1186/1741-7007-9-5.
45. **Vidi PA, Chemel BR, Hu CD, Watts VJ.** 2008. Ligand-dependent oligomerization of dopamine D(2) and adenosine A(2A) receptors in living neuronal cells. Mol. Pharmacol. **74:**544–551. http://dx.doi.org/10.1124/mol.108.047472.
46. **Guo Z, Chen LM, Zeng H, Gomez JA, Plowden J, Fujita T, Katz JM, Donis RO, Sambhara S.** 2007. NS1 protein of influenza A virus inhibits the function of intracytoplasmic pathogen sensor, RIG-I. Am. J. Respir. Cell Mol. Biol. **36:**263–269. http://dx.doi.org/10.1165/rcmb.2006-0283RC.
47. **Mibayashi M, Martinez-Sobrido L, Loo YM, Cardenas WB, Gale M, Jr, Garcia-Sastre A.** 2007. Inhibition of retinoic acid-inducible gene I-mediated induction of beta interferon by the NS1 protein of influenza A virus. J. Virol. **81:**514–524. http://dx.doi.org/10.1128/JVI.01265-06.
48. **Opitz B, Rejaibi A, Dauber B, Eckhard J, Vinzing M, Schmeck B, Hippenstiel S, Suttorp N, Wolff T.** 2007. IFNbeta induction by influenza A virus is mediated by RIG-I which is regulated by the viral NS1 protein. Cell. Microbiol. **9:**930–938. http://dx.doi.org/10.1111/j.1462-5822.2006.00841.x.
49. **de la Luna S, Fortes P, Beloso A, Ortin J.** 1995. Influenza virus NS1 protein enhances the rate of translation initiation of viral mRNAs. J. Virol. **69:**2427–2433.
50. **Marión RM, Aragon T, Beloso A, Nieto A, Ortin J.** 1997. The N-terminal half of the influenza virus NS1 protein is sufficient for nuclear retention of mRNA and enhancement of viral mRNA translation. Nucleic Acids Res. **25:**4271–4277. http://dx.doi.org/10.1093/nar/25.21.4271.
51. **Nivitchanyong T, Yongkiettrakul S, Kramyu J, Pannengpetch S, Wanasen N.** 2011. Enhanced expression of secretable influenza virus neuraminidase in suspension mammalian cells by influenza virus nonstructural protein 1. J. Virol. Methods **178:**44–51. http://dx.doi.org/10.1016/j.jviromet.2011.08.010.
52. **Li G, Zhang J, Tong X, Liu W, Ye X.** 2011. Heat shock protein 70 inhibits the activity of influenza A virus ribonucleoprotein and blocks the replication of virus in vitro and in vivo. PLoS One **6:**e16546. http://dx.doi.org/10.1371/journal.pone.0016546.
53. **Manzoor R, Kuroda K, Yoshida R, Tsuda Y, Fujikura D, Miyamoto H, Kajihara M, Kida H, Takada A.** 2014. Heat shock protein 70 modulates influenza A virus polymerase activity. J. Biol. Chem. **289:**7599–7614. http://dx.doi.org/10.1074/jbc.M113.507798.
54. **Ge X, Rameix-Welti MA, Gault E, Chase G, dos Santos Afonso E, Picard D, Schwemmle M, Naffakh N.** 2011. Influenza virus infection induces the nuclear relocalization of the Hsp90 co-chaperone p23 and inhibits the glucocorticoid receptor response. PLoS One **6:**e23368. http://dx.doi.org/10.1371/journal.pone.0023368.
55. **Ohman T, Rintahaka J, Kalkkinen N, Matikainen S, Nyman TA.** 2009. Actin and RIG-I/MAVS signaling components translocate to mitochondria upon influenza A virus infection of human primary macrophages. J. Immunol. **182:**5682–5692. http://dx.doi.org/10.4049/jimmunol.0803093.
56. **Wu W, Zhang W, Booth JL, Metcalf JP.** 2012. Influenza A(H1N1)pdm09 virus suppresses RIG-I initiated innate antiviral responses in the human lung. PLoS One **7:**e49856. http://dx.doi.org/10.1371/journal.pone.0049856.
57. **Morosky SA, Zhu J, Mukherjee A, Sarkar SN, Coyne CB.** 2011. Retinoic acid-induced gene-I (RIG-I) associates with nucleotide-binding oligomerization domain-2 (NOD2) to negatively regulate inflammatory signaling. J. Biol. Chem. **286:**28574–28583. http://dx.doi.org/10.1074/jbc.M111.227942.
58. **Mukherjee A, Morosky SA, Shen L, Weber CR, Turner JR, Kim KS, Wang T, Coyne CB.** 2009. Retinoic acid-induced gene-1 (RIG-I) associates with the actin cytoskeleton via caspase activation and recruitment domain-dependent interactions. J. Biol. Chem. **284:**6486–6494. http://dx.doi.org/10.1074/jbc.M807547200.
59. **Leverrier Y, Ridley AJ.** 2001. Apoptosis: caspases orchestrate the ROCK 'n' bleb. Nat. Cell Biol. **3:**E91–E93. http://dx.doi.org/10.1038/35070151.
60. **Pichlmair A, Schulz O, Tan CP, Rehwinkel J, Kato H, Takeuchi O, Akira S, Way M, Schiavo G, Reis e Sousa C.** 2009. Activation of MDA5 requires higher-order RNA structures generated during virus infection. J. Virol. **83:**10761–10769. http://dx.doi.org/10.1128/JVI.00770-09.
61. **Pauli EK, Schmolke M, Wolff T, Viemann D, Roth J, Bode JG, Ludwig S.** 2008. Influenza A virus inhibits type I IFN signaling via NF-kappaB-dependent induction of SOCS-3 expression. PLoS Pathog. **4:**e1000196. http://dx.doi.org/10.1371/journal.ppat.1000196.
62. **Eisenächer K, Krug A.** 2012. Regulation of RLR-mediated innate immune signaling—it is all about keeping the balance. Eur. J. Cell Biol. **91:**36–47. http://dx.doi.org/10.1016/j.ejcb.2011.01.011.
63. **Boivin S, Cusack S, Ruigrok RW, Hart DJ.** 2010. Influenza A virus polymerase: structural insights into replication and host adaptation mechanisms. J. Biol. Chem. **285:**28411–28417. http://dx.doi.org/10.1074/jbc.R110.117531.
64. **Boulo S, Akarsu H, Ruigrok RW, Baudin F.** 2007. Nuclear traffic of influenza virus proteins and ribonucleoprotein complexes. Virus Res. **124:**12–21. http://dx.doi.org/10.1016/j.virusres.2006.09.013.
65. **Nagata K, Kawaguchi A, Naito T.** 2008. Host factors for replication and transcription of the influenza virus genome. Rev. Med. Virol. **18:**247–260. http://dx.doi.org/10.1002/rmv.575.
66. **van de Sandt CE, Kreijtz JH, Rimmelzwaan GF.** 2012. Evasion of influenza A viruses from innate and adaptive immune responses. Viruses **4:**1438–1476. http://dx.doi.org/10.3390/v4091438.
67. **Shapira SD, Gat-Viks I, Shum BO, Dricot A, de Grace MM, Wu L, Gupta PB, Hao T, Silver SJ, Root DE, Hill DE, Regev A, Hacohen N.** 2009. A physical and regulatory map of host-influenza interactions reveals pathways in H1N1 infection. Cell **139:**1255–1267. http://dx.doi.org/10.1016/j.cell.2009.12.018.
68. **Baudin F, Bach C, Cusack S, Ruigrok RW.** 1994. Structure of influenza virus RNP. I. Influenza virus nucleoprotein melts secondary structure in panhandle RNA and exposes the bases to the solvent. EMBO J. **13:**3158–3165.
69. **Ye Q, Guu TS, Mata DA, Kuo RL, Smith B, Krug RM, Tao YJ.** 2012. Biochemical and structural evidence in support of a coherent model for

the formation of the double-helical influenza A virus ribonucleoprotein. mBio **4:**e00467-12. http://dx.doi.org/10.1128/mBio.00467-12.

70. **Weber M, Gawanbacht A, Habjan M, Rang A, Borner C, Schmidt AM, Veitinger S, Jacob R, Devignot S, Kochs G, Garcia-Sastre A, Weber F.** 2013. Incoming RNA virus nucleocapsids containing a 5′-triphosphorylated genome activate RIG-I and antiviral signaling. Cell Host Microbe **13:**336–346. http://dx.doi.org/10.1016/j.chom.2013.01.012.
71. **Guan Y, Shortridge KF, Krauss S, Webster RG.** 1999. Molecular characterization of H9N2 influenza viruses: were they the donors of the "internal" genes of H5N1 viruses in Hong Kong? Proc. Natl. Acad. Sci. U. S. A. **96:**9363–9367. http://dx.doi.org/10.1073/pnas.96.16.9363.
72. **Gao R, Cao B, Hu Y, Feng Z, Wang D, Hu W, Chen J, Jie Z, Qiu H, Xu K, Xu X, Lu H, Zhu W, Gao Z, Xiang N, Shen Y, He Z, Gu Y, Zhang Z, Yang Y, Zhao X, Zhou L, Li X, Zou S, Zhang Y, Li X, Yang L, Guo J, Dong J, Li Q, Dong L, Zhu Y, Bai T, Wang S, Hao P, Yang W, Zhang Y, Han J, Yu H, Li D, Gao GF, Wu G, Wang Y, Yuan Z, Shu Y.** 2013. Human infection with a novel avian-origin influenza A (H7N9) virus. N. Engl. J. Med. **368:**1888–1897. http://dx.doi.org/10.1056/NEJMoa1304459.
73. **Chen H, Yuan H, Gao R, Zhang J, Wang D, Xiong Y, Fan G, Yang F, Li X, Zhou J, Zou S, Yang L, Chen T, Dong L, Bo H, Zhao X, Zhang Y, Lan Y, Bai T, Dong J, Li Q, Wang S, Zhang Y, Li H, Gong T, Shi Y, Ni X, Li J, Zhou J, Fan J, Wu J, Zhou X, Hu M, Wan J, Yang W, Li D, Wu G, Feng Z, Gao GF, Wang Y, Jin Q, Liu M, Shu Y.** 2014. Clinical and epidemiological characteristics of a fatal case of avian influenza A H10N8 virus infection: a descriptive study. Lancet **383:**714–721. http://dx.doi.org/10.1016/S0140-6736(14)60111-2.
74. **Jorba N, Juarez S, Torreira E, Gastaminza P, Zamarreno N, Albar JP, Ortin J.** 2008. Analysis of the interaction of influenza virus polymerase complex with human cell factors. Proteomics **8:**2077–2088. http://dx.doi.org/10.1002/pmic.200700508.
75. **Tafforeau L, Chantier T, Pradezynski F, Pellet J, Mangeot PE, Vidalain PO, Andre P, Rabourdin-Combe C, Lotteau V.** 2011. Generation and comprehensive analysis of an influenza virus polymerase cellular interaction network. J. Virol. **85:**13010–13018. http://dx.doi.org/10.1128/JVI.02651-10.
76. **Bortz E, Westera L, Maamary J, Steel J, Albrecht RA, Manicassamy B, Chase G, Martinez-Sobrido L, Schwemmle M, Garcia-Sastre A.** 2011. Host- and strain-specific regulation of influenza virus polymerase activity by interacting cellular proteins. mBio **2**(4):e00151-11. http://dx.doi.org/10.1128/mBio.00151-11.
77. **Momose F, Basler CF, O'Neill RE, Iwamatsu A, Palese P, Nagata K.** 2001. Cellular splicing factor RAF-2p48/NPI-5/BAT1/UAP56 interacts with the influenza virus nucleoprotein and enhances viral RNA synthesis. J. Virol. **75:**1899–1908. http://dx.doi.org/10.1128/JVI.75.4.1899-1908.2001.
78. **Wisskirchen C, Ludersdorfer TH, Muller DA, Moritz E, Pavlovic J.** 2011. The cellular RNA helicase UAP56 is required for prevention of double-stranded RNA formation during influenza A virus infection. J. Virol. **85:**8646–8655. http://dx.doi.org/10.1128/JVI.02559-10.
79. **Chen G, Liu CH, Zhou L, Krug RM.** 2014. Cellular DDX21 RNA helicase inhibits influenza A virus replication but is counteracted by the viral NS1 protein. Cell Host Microbe **15:**484–493. http://dx.doi.org/10.1016/j.chom.2014.03.002.
80. **Shigemoto T, Kageyama M, Hirai R, Zheng J, Yoneyama M, Fujita T.** 2009. Identification of loss of function mutations in human genes encoding RIG-I and MDA5: implications for resistance to type I diabetes. J. Biol. Chem. **284:**13348–13354. http://dx.doi.org/10.1074/jbc.M809449200.
81. **Sumpter R, Jr, Loo YM, Foy E, Li K, Yoneyama M, Fujita T, Lemon SM, Gale M, Jr.** 2005. Regulating intracellular antiviral defense and permissiveness to hepatitis C virus RNA replication through a cellular RNA helicase, RIG-I. J. Virol. **79:**2689–2699. http://dx.doi.org/10.1128/JVI.79.5.2689-2699.2005.
82. **Binder M, Kochs G, Bartenschlager R, Lohmann V.** 2007. Hepatitis C virus escape from the interferon regulatory factor 3 pathway by a passive and active evasion strategy. Hepatology **46:**1365–1374. http://dx.doi.org/10.1002/hep.21829.